Received: 24 March 2023 | Revised: 7 July 2023 | Accepted: 28 July 2023

DOI: 10.1002/hbm.26450

RESEARCH ARTICLE

WILEY

Single-subject cortical morphological brain networks across the adult lifespan

Jingxuan Ruan[1] | Ningkai Wang[2] | Junle Li[2] | Jing Wang[2] | Qihong Zou[3] | Yating Lv[4] | Han Zhang[1] | Jinhui Wang[2,5,6,7]

[1]School of Electronics and Information Technology, South China Normal University, Foshan, China

[2]Institute for Brain Research and Rehabilitation, South China Normal University, Guangzhou, China

[3]Center for MRI Research, Academy for Advanced Interdisciplinary Studies, Peking University, Beijing, China

[4]Institute of Psychological Sciences, Hangzhou Normal University, Zhejiang, Hangzhou, China

[5]Key Laboratory of Brain, Cognition and Education Sciences, Ministry of Education, Beijing, China

[6]Center for Studies of Psychological Application, South China Normal University, Guangzhou, China

[7]Guangdong Key Laboratory of Mental Health and Cognitive Science, South China Normal University, Guangzhou, China

Correspondence

Jinhui Wang, Institute for Brain Research and Rehabilitation, South China Normal University, Guangzhou, 510631, China.
Email: jinhui.wang.1982@m.scnu.edu.cn

Han Zhang, School of Electronics and Information Technology, South China Normal University, Foshan, 528200, China.
Email: zhanghan@scnu.edu.cn

Funding information

Key Realm R&D Program of Guangdong Province, Grant/Award Number: 2019B030335001; Key Realm R&D Program of Guangzhou, Grant/Award Number: 202007030005; National Natural Science Foundation of China, Grant/Award Number: 81922036; National Social Science Fund of China; National Social Science Foundation of China, Grant/Award Number: 20&ZD296

Abstract

Age-related changes in focal cortical morphology have been well documented in previous literature; however, how interregional coordination patterns of the focal cortical morphology reorganize with advancing age is not well established. In this study, we performed a comprehensive analysis of the topological changes in single-subject morphological brain networks across the adult lifespan. Specifically, we constructed four types of single-subject morphological brain networks for 650 participants (aged from 18 to 88 years old), and characterized their topological organization using graph-based network measures. Age-related changes in the network measures were examined via linear, quadratic, and cubic models. We found profound age-related changes in global small-world attributes and efficiency, local nodal centralities, and interregional similarities of the single-subject morphological brain networks. The age-related changes were mainly embodied in cortical thickness networks, involved in frontal regions and highly connected hubs, concentrated on short-range connections, characterized by linear changes, and susceptible to connections between limbic, frontoparietal, and ventral attention networks. Intriguingly, nonlinear (i.e., quadratic or cubic) age-related changes were frequently found in the insula and limbic regions, and age-related cubic changes preferred long-range morphological connections. Finally, we demonstrated that the morphological similarity in cortical thickness between two frontal regions mediated the relationship between age and cognition measured by Cattell scores. Taken together, these findings deepen our understanding of adaptive changes of the human brain with advancing age, which may account for interindividual variations in behaviors and cognition.

KEYWORDS

anatomical distance, hub, lifespan, morphological brain network, structural MRI

Jingxuan Ruan and Ningkai Wang contributed equally to this work.

1 | INTRODUCTION

The human brain is a complex system that can be modeled as interconnected networks in vivo from multimodal magnetic resonance imaging (MRI) data at different temporal and spatial scales. To date, several nontrivial organizational principles are universally observed to govern the networks for facilitating segregated and integrated information processing, including small-worldness, rich-club structure, and modular organization (Bullmore & Sporns, 2009; Liao et al., 2017; Sporns & Betzel, 2016; van den Heuvel & Sporns, 2013). Moreover, the nontrivial network architecture undergoes dynamic reconfiguration across the human lifespan to accommodate behaviors and intelligence (Cao et al., 2017; Zuo et al., 2017). However, the existing knowledge on the brain network changes across the human lifespan is mainly from network analyses of functional and diffusion MRI. Little is known regarding age-related changes in morphological brain networks derived from structural MRI, which have become an important way for brain connectome studies.

Historically, morphological brain networks are mainly derived from population-based morphological covariance methods by calculating Pearson correlation in regional morphology (e.g., cortical thickness or gray matter volume) across a cohort of participants (Bassett et al., 2008; He et al., 2007). Despite successful application to studies of age-related changes (Chen et al., 2011; Váša et al., 2018; Wu et al., 2012), the population-based methods ignore inter-individual variance, and thus fail to uncover detailed, continuous changes with increasing age. By contrast, the recent advent of single-subject morphological brain network approaches makes it possible to examine age-related changes at a finer scale (Kong et al., 2015; Li et al., 2017; Li et al., 2021; Seidlitz et al., 2018; Tijms et al., 2012; Wang et al., 2016). Using the newly developed approaches, two previous studies have explored early cortical development of the neonatal brain (Fenchel et al., 2020; Galdi et al., 2020). More recently, two large sample studies further examined single-subject morphological brain networks across the adult lifespan (Shigemoto et al., 2023; Wang et al., 2022). However, these studies constructed single-subject morphological brain networks either based on a single morphological feature (i.e., gray matter volume) or by integrating multiple features into a single model. It is thus still unclear how single-subject morphological brain networks derived from different morphological features differentially change with advancing age. Given our previous findings that single-subject morphological brain networks constructed with different morphological features exhibited distinct wiring patterns (Li et al., 2021) and different sensitivities in uncovering disease-related alterations (Lv et al., 2021), a better understanding of age-related changes in the brain may benefit from a more comprehensive study of different types of single-subject morphological brain networks.

In this study, we aimed to utilize single-subject morphological brain network methods to systemically investigate age-related changes in multiple morphological features for 650 participants (aged from 18 to 88 years old) from a publicly available dataset of the Cambridge Centre for Aging and Neuroscience (Cam-CAN). The single-subject morphological brain networks were constructed with our previous approaches established for four widely used morphological features of fractal dimension (FD), gyrification index (GI), sulcal depth (SD), and cortical thickness (CT) (Li et al., 2021). After topologically characterizing each type of the single-subject morphological brain networks with graph-based approaches, age-related changes were examined via linear and nonlinear models at global, nodal, and connectional levels. Finally, associations of the age-related changes in the single-subject morphological brain networks were examined with individual cognitive abilities measured by the Cattell scores.

2 | MATERIALS AND METHODS

2.1 | Participants and data acquisition

A total of 652 healthy participants were included in the large-scale Cam-CAN collaborative research project, launched in October 2010 (http://www.mrc-cbu.cam.ac.uk/datasets/camcan/). This project aimed to use epidemiological, cognitive, and neuroimaging data to understand how individuals can best retain cognitive abilities into old age (Cam-CAN et al., 2014; Taylor et al., 2017). Informed consent was obtained from each participant and ethical approval for the procedures for data collection and sharing was obtained from the Cambridgeshire 2 (now East of England-Cambridge Central) Research Ethics Committee. After excluding two participants according to our quality control procedures (see below), a total of 650 participants were included in the final analyses (age range, 18–88 years old; mean age, 54.3 ± 18.6 years old; 320 males) (Figure 1). All participants were cognitively healthy with a 24 or higher score on the Mini-Mental State Examination, had normal or corrected-to-normal vision and hearing, were free of MRI or MEG contraindications, and had no history of drug or alcohol abuse or any neurological or serious psychiatric conditions.

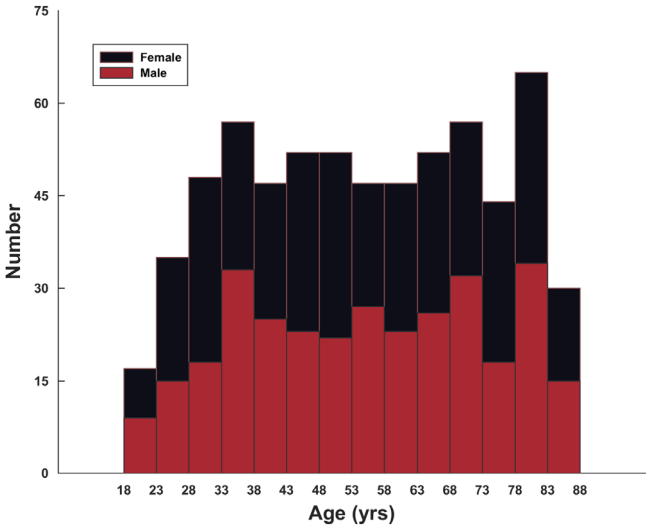

FIGURE 1 Histogram showing age and sex distributions of the participants.

The Cam-CAN project collected multiple modalities of neuroimaging data, among which high-resolution 3D T1-weighted structural MRI images were used in this study. The images were scanned in a Siemens Trio 3 T scanner with a 32-channel head-coil. Specifically, the magnetization-prepared rapid gradient-echo sequence was used to acquire individual structural MRI images with the following parameters: repetition time = 2250 ms; echo time = 2.99 ms; inversion time = 900 ms; flip angle = 9°; field of view = 256 × 240 × 192 mm^3; voxel size = 1 × 1 × 1 mm^3; acceleration factor = 2; and acquisition time = 4 min and 32 s.

In addition to the structural MRI images, the standard form of the Cattell Culture Fair, Scale 2 Form A was used in this study to examine the associations of age-related changes in single-subject morphological brain networks with cognition. The Cattell test is a pen-and-paper test that consists of four nonverbal subtests: completing a sequence of drawings (series completion subtest), picking a drawing that is different from other drawings (classification subtest), completing a matrix of patterns (matrix subtest), and picking geometric designs that fulfill a specific given condition (conditions subtest). After the four subtests, each participant got a score ranging from 0 to 46.

2.2 | Quality control procedures

All structural MRI images were checked for quality control by semi-automated scripts monitored by the Cam-CAN methods team (Taylor et al., 2017). Further, we checked the results of image segmentation via the modules "Slice Display" and "Surface Data Homogeneity" in the CAT12 toolbox. One participant (sub-CC620821) failed in the tissue segmentation. In addition, another participant (sub-CC320651) was excluded due to failure in the extraction of vertex-wise GI.

2.3 | Preprocessing of structural MRI images

As in our previous studies (Li et al., 2021; Lv et al., 2021), all structural MRI images were preprocessed using the CAT12 toolbox (version r1113, http://www.neuro.uni-jena.de/cat/). There is a growing number of studies demonstrating that the CAT12 can be regarded as a considerable alternative to FreeSurfer for accurate and reliable estimates of CT (Ay et al., 2022; Righart et al., 2017; Seiger et al., 2018). Particularly, the CAT12 offers a volume-based approach for estimating CT without extensive reconstruction of cortical surface, and thus is timesaving. This feature is important for this study given our large sample size. Briefly, after tissue segment of each structural MRI image, CT was estimated using a fast and reliable projection-based thickness method, and FD, GI, and SD were estimated based on spherical harmonic reconstructions. Specifically, FD was calculated as the slope of a logarithmic plot of surface area versus the maximum l-value (Yotter et al., 2011), GI was computed as the absolute mean curvature (Luders et al., 2006), and SD was defined as the Euclidean distance between the central surface and its convex hull. The resulting vertex-wise morphological maps were subsequently resampled into the common fsaverage template, and smoothed using a Gaussian kernel. Spatial smoothing is previously demonstrated to increase test–retest reliability of single-subject morphological brain networks (Wang et al., 2016). Specifically, according to the recommendations of the CAT12 manual, individual CT maps were smoothed using a Gaussian kernel with a 15-mm full width at half maximum (FWHM), while individual FD, GI, and SD maps were smoothed using a Gaussian kernel with a 25-mm FWHM. The usage of larger smoothing kernel sizes for the FD, GI, and SD maps is due to the underlying nature of these folding measures that reflect contributions from both sulci and gyri. Therefore, the filter size should exceed the distance between a gyral crown and a sulcal fundus.

To test whether the different smoothing kernel sizes affected our findings, we re-smoothed individual CT maps using a Gaussian kernel with a 25-mm FWHM. High within-subject correlations were observed for the resulting single-subject morphological brain networks ($r = .532 \pm .050$). These findings imply limited effects of different smoothing kernel sizes on our results given that all topological attributes were calculated for binary networks in this study (see below for details).

2.4 | Construction of single-subject morphological similarity matrix

In this study, we constructed four types of single-subject morphological similarity matrices for each participant based on different morphological indices (FD, GI, SD, and CT). In the matrices, nodes represented brain regions and edges represented interregional similarities in regional morphology.

2.4.1 | Definition of network nodes

To define nodes, we employed a widely used Destrieux atlas (Destrieux et al., 2010) to divide the cerebral cortex into 148 regions of interest (ROIs). Each ROI was a node in the morphological similarity matrices. Our previous studies demonstrated that different choices of parcellation atlas significantly affected the topological descriptions of single-subject cortical morphological brain networks, and higher resolution atlases yielded higher test–retest reliability (Li et al., 2021; Yin et al., 2023). However, higher resolution atlases (i.e., more network nodes) were accompanied with more computational demands. In this study, we chose the Destrieux atlas, which provided an acceptable trade-off between test–retest reliability and computational cost.

2.4.2 | Definition of network edges

To estimate edges between the nodes, we calculated interregional morphological similarity in the distribution of regional morphology in terms of the Jensen-Shannon divergence (JSD) (Li et al., 2021). The JSD, a variant of Kullback–Leibler divergence (KLD), is a measure of

the distance between two probability distributions. Our previous studies have found that compared with the KLD, the JSD can yield more test–retest reliable estimation for single-subject cortical morphological brain networks (Li et al., 2021; Yin et al., 2023). First, for each morphological index we extracted values of all vertices within each ROI. Then, a probability density estimate was obtained for each ROI and each morphological index using a normal kernel function (MATLAB function, ksdensity). Each of the resulting probability density estimates was further converted to a probability distribution function (PDF). For two regional PDFs P and Q, the JSD is calculated as:

$$\mathrm{KLD}\left(P\middle\|Q\right) = \sum_{i=1}^{n} P(i)\, log\frac{P(i)}{Q(i)},$$

$$\mathrm{JSD}\left(P\middle\|Q\right) = \frac{1}{2}\mathrm{KLD}\left(P\middle\|\frac{1}{2}(P+Q)\right) + \frac{1}{2}\mathrm{KLD}\left(Q\middle\|\frac{1}{2}(P+Q)\right),$$

where n is the number of sampling points during the probability density estimate. According to our previous study (Wang et al., 2016), n was set to 2^8 for each ROI no matter how many vertices the ROIs included. Notably, the bilateral pericallosal sulci were excluded due to a limited number of vertices in them. Finally, the morphological similarity was defined as the square root of the JSD, followed by a subtraction from 1. After the procedures mentioned above, a total of four 146 × 146 morphological similarity matrices were obtained for each participant. In the matrices, the value of interregional morphological similarity ranged from 0 to 1, with 0 and 1 denoting that two regional PDFs are completely different and exactly the same, respectively.

2.5 | Network analysis

2.5.1 | Threshold selection

Before topological characterization of the morphological similarity matrices derived above, a sparsity-based thresholding procedure was used to convert the matrices to binary networks. Compared with weighted networks, binary networks are demonstrated to yield higher test–retest reliability for graph-based topological measures of human brain networks (Wang et al., 2011; Wang et al., 2016; Yin et al., 2023). Sparsity is defined as the ratio of the number of actual edges divided by the maximum possible number of edges in a network. The sparsity-based thresholding method thus ensures the same number of edges across participants and in each type of morphological brain networks. Owing to the lack of a definitive way to select a single sparsity, we thresholded each matrix to generate a series of binary networks in a consecutive sparsity range from 0.04 to 0.4 with an interval of 0.02. The lower limit of the sparsity range was determined to ensure that the resulting binary networks were estimable for the small-world attributes (Watts & Strogatz, 1998). That is, the average degree over all nodes should be larger than 2 × log(N), where N denoted the number of nodes (i.e., 146 in this study) in the networks. The upper limit of the sparsity range was empirically chosen to guarantee that the resulting binary networks had sparse properties (Achard & Bullmore, 2007; Wang et al., 2009).

2.5.2 | Network parameter calculation

We calculated four global (clustering coefficient, C_p; characteristic path length, L_p; local efficiency, E_{loc}; global efficiency, E_{glob}) and three nodal centrality (degree, k_i; efficiency, e_i; nodal betweenness, b_i) measures to topologically characterize the morphological brain networks at each sparsity. Formulas, usages, and explanations of these measures can be found elsewhere (Rubinov & Sporns, 2010; Wang et al., 2011). Since all network measures were calculated as functions of the sparsity, we further computed the area under the curve (AUC; i.e., the integral over the entire sparsity range) for each measure to provide a summarized scalar for subsequent statistical analyses. All the network analyses were performed with the GRETNA toolbox (Wang et al., 2015).

2.5.3 | Definition of hubs

For each participant, brain hubs were first defined as regions with values in the top 10% for each nodal centrality measure of each type of morphological brain network. By counting the times of each region as a hub among all participants, 12 (3 nodal centrality measures × 4 morphological indices) hub probability maps were then obtained. For each hub probability map, regions with values in the top 10% of the probability were identified as group-level brain hubs.

2.6 | Statistical models for detecting age-related changes

The general linear model was used to explore age-related changes in morphological brain networks. Specifically, for each type of morphological brain network, three models were used to separately examine linear, quadratic, and cubic age-related changes in morphological similarity between each pair of ROIs, each global network measure, each nodal centrality measure of each ROI, the mean of each nodal centrality measure across group-level hubs, and the mean of each nodal centrality measure across group-level non-hubs as follows:

$$Y = \beta_0 + \beta_1 \times \mathrm{age} + \beta_2 \times \mathrm{sex},$$

$$Y = \beta_0 + \beta_1 \times \mathrm{age} + \beta_2 \times \mathrm{age}^2 + \beta_3 \times \mathrm{sex},$$

$$Y = \beta_0 + \beta_1 \times age + \beta_2 \times \mathrm{age}^2 + \beta_3 \times \mathrm{age}^3 + \beta_4 \times \mathrm{sex}.$$

To determine the best-fitting model, the Akaike's information criterion (AIC) was used (Akaike, 1974; Hurvich & Tsai, 1989), which was calculated as:

$$AIC = 2h - 2ln\left(\hat{L}\right),$$

where h is the number of estimated parameters in a model, and $\hat{L}$ is the maximum value of the likelihood function for the model. A smaller AIC value means a better trade-off between the goodness of fit and the number of estimated parameters. If a quadratic model was determined, the peak point of age was calculated as:

$$Age_{peak} = \frac{-\beta_1}{2\beta_2}.$$

If a cubic model was determined, the inflection point of age was calculated as:

$$Age_{inflection} = -\frac{\beta_2}{3\beta_3}.$$

When $\beta_2^2 - 3 \times \beta_1 \times \beta_3 > 0$, the stationary points of age were further calculated as:

$$Age_{stationary} = \frac{-\beta_2 \pm \sqrt{\beta_2^2 - 3\beta_1 \times \beta_3}}{3\beta_3}.$$

For each type of morphological brain networks, the false discovery rate (FDR) procedure was used to correct for multiple comparisons for analyses of interregional morphological similarity (across connections), global network organization (across measures), and local network organization (across regions and nodal centrality measures).

The above procedures were also used to examine the age-related changes in local morphology (i.e., regional mean of each morphological feature).

2.7 | Effects of anatomical distance on age-related changes in single-subject morphological brain networks

To examine whether the age-related changes in morphological brain networks were dependent on anatomical distance, we first calculated an interregional anatomical distance matrix for each participant. The anatomical distance between two regions was approximately computed as the mean Euclidean distance across all pairs of vertices belonging to the two regions. The individual anatomical distance matrices were then averaged to generate a group-level anatomical distance matrix, based on which we compared the distances between morphological connections with and without age-related changes. Given the huge differences in the numbers of the two sets of connections (FD network: 1154 vs. 9431; GI network: 518 vs. 10067; SD network: 2125 vs. 8460; CT network: 3588 vs. 6997; see Results), we performed the following statistical analyses. We separately selected 1154, 518, 2125, and 3588 edges from the group-level anatomical distance matrix randomly and calculated their mean distances. This procedure was implemented 100,000 times to generate four empirical null distributions, each of which was used to determine a two-tailed p-value, indicating the deviation of the real observation (i.e., mean anatomical distance across the connections showing age-related changes) of each type of morphological brain network from chance operations. Similar analyses were also performed for morphological connections showing age-related linear, quadratic, and cubic changes, respectively.

2.8 | Effects of cortical modules on age-related changes in single-subject morphological brain networks

To examine whether the age-related changes in morphological brain networks were susceptible to specific cortical modules, we first assigned each ROI to one of the seven modules (Thomas Yeo et al., 2011): default mode network (DMN), frontoparietal network (FPN), dorsal attention network (DAN), ventral attention network (VAN), limbic network (LN), visual network (VN) and somatomotor network (SMN). To achieve this, we calculated the proportions of vertices belonging to different modules for each ROI, and an ROI was assigned to the module with the highest proportion if the proportion was larger than 50% and was at least 20% more than the second-highest proportion. The ROIs failing to meet the criteria were excluded from this analysis (27). Subsequently, we counted the numbers of morphological connections showing significant age-related changes within each and between each pair of modules. To determine whether the observed numbers statistically deviated from chance operations, we randomly selected the same numbers of morphological connections 100,000 times and recorded their distributions in the context of the seven modules. Based on the resulting empirical null distributions, a one-tailed p-value was finally obtained for each module and each pair of modules, which indicated whether the morphological connections showing age-related changes were selectively involved in specific modules or between specific pairs of modules. The FDR procedure was used to correct for multiple comparisons.

2.9 | Association of age-related changes in single-subject morphological brain networks with cognition

For morphological measures showing age-related changes, we computed their Pearson correlations with the Cattell scores after removing the effects of sex via general linear models. However, the correlations may be driven by age-related effects, since we found a significantly negative quadratic trajectory with the increase of age for the Cattell scores. Thus, we re-computed the correlations after removing additional effects of age. This allows identifying morphological measures that can account for significant variance in the Cattell scores that was independent of age-related changes (Kievit et al., 2014; Madden et al., 2008). The FDR procedure was used to

correct for multiple comparisons at each analysis level of local morphology, interregional morphological similarity, global and local network organization.

3 | RESULTS

3.1 | Age-related changes in global measures of single-subject morphological brain networks

Significant age-related changes in global network organization of morphological brain networks were observed only for the CT networks ($p < .05$, FDR corrected; Figure 2).

3.1.1 | CT networks

Clustering coefficient ($p < .001$) and local efficiency ($p < .001$) decreased linearly with the increase of age, while characteristic path length ($\sim -$ shape: $p = .004$; inflection point: 54; stationary points: 41 and 67) and global efficiency (inverted $\sim -$ shape: $p = .006$; inflection point: 54; stationary points: 41 and 67) showed cubic age-related trajectories.

3.2 | Age-related changes in nodal centrality measures of single-subject morphological brain networks

Significant age-related changes in nodal centrality measures were observed for all types of morphological brain networks, particularly the SD and CT networks ($p < .05$, FDR corrected; Figures S1). In general, the changes were mainly characterized by linear changes, and involved in frontal and temporal regions regardless of the type of morphological brain networks.

3.2.1 | FD networks

Significant age-related changes (linear: 35, 77.8%; quadratic: 8, 17.8%; cubic: 2, 4.4%) were observed on at least one nodal centrality measure of 26 regions for the FD networks (frontal: 9, 34.6%).

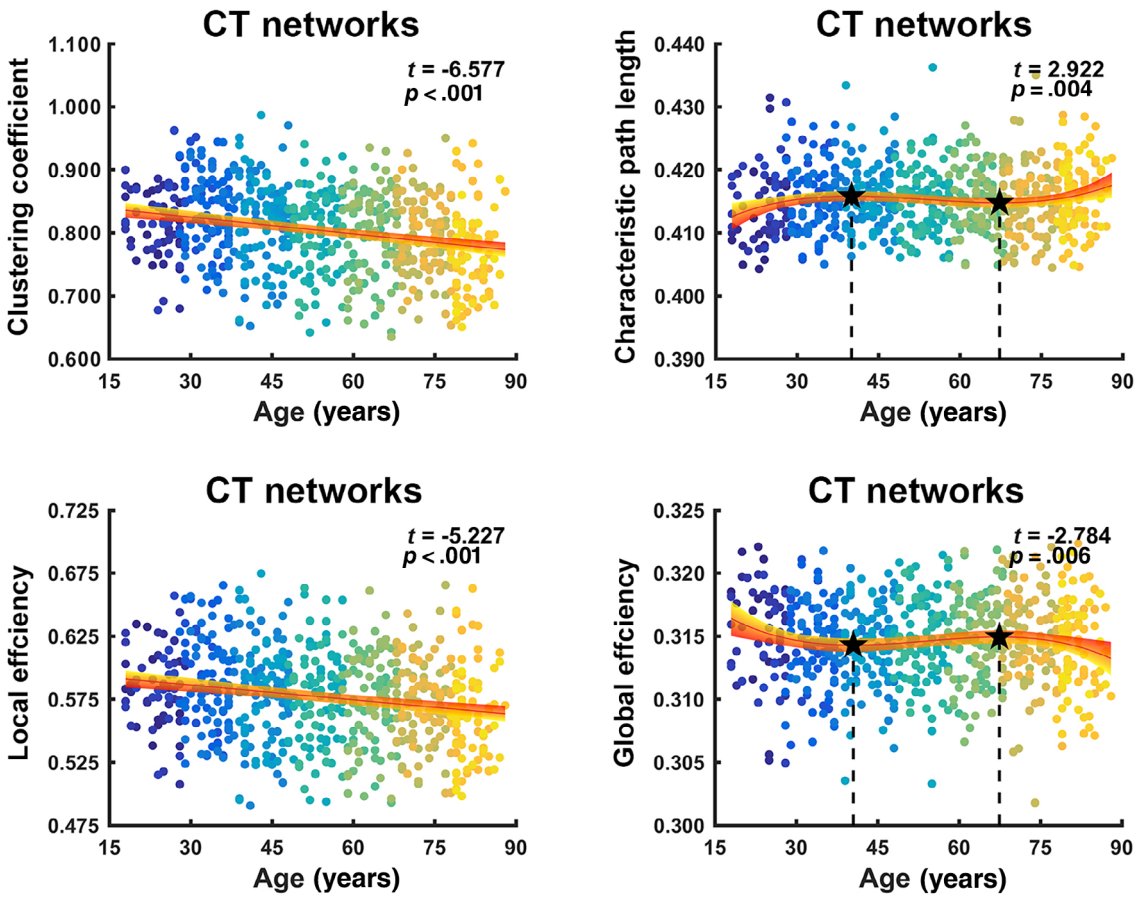

FIGURE 2 Age-related changes in global network measures. Significant age-related changes were observed only in the CT networks. Shades denote 95% confidence intervals of model fitness. Black stars denote stationary points of age in cubic models. CT, cortical thickness.

3.2.2 | GI networks

Significant age-related changes (linear: 19, 70.4%; quadratic: 5, 18.5%; cubic: 3, 1.1%) were observed on at least one nodal centrality measure of 15 regions for the GI networks (temporal: 5, 33.3%).

3.2.3 | SD networks

Significant age-related changes (linear: 46, 74.2%; quadratic: 9, 14.5%; cubic: 7, 11.3%) were observed on at least one nodal centrality measure of 36 regions for the SD networks (frontal: 7, 19.4%; limbic: 7, 19.4%; insula: 6, 16.7%).

3.2.4 | CT networks

Significant age-related changes (linear: 75, 55.6%; quadratic: 38, 28.1%; cubic: 22, 16.3%) were observed on at least one nodal centrality measure of 73 regions for the CT networks (frontal: 27, 37.0%).

All age-related changes in nodal centrality measures are further summarized in Figure 3 and Table S1. We noted that (1) both linear increases and decreases with age were observed for each type of morphological brain networks; (2) quadratic and cubic age-related changes were mainly found in the CT networks, and the regions were mainly involved in the insula and limbic regions (e.g., the cingulate gyrus and parahippocampal gyrus); and (3) several regions were consistently found to show age-related changes in multiple nodal centrality measures and different types of morphological brain networks, such as the left suborbital sulcus, the posterior-ventral part of the right cingulate gyrus, the inferior circular sulcus of the left insula, the right anterior cingulate cortex, and the right parahippocampal gyrus.

3.3 | Age-related changes in hubs of single-subject morphological brain networks

Figure 4 (the first three rows) shows the hub probability map for each nodal centrality measure of each type of morphological brain networks over all participants. We found that hub probabilities exhibited very high spatial correlations across different nodal centrality measures for the same type of morphological brain networks ($r = .874 \pm .097$) while low correlations were observed between different types of morphological brain networks ($r = .342 \pm .107$) (Figure 5). Accordingly, hub regions with the highest probabilities (15, 10%) differed largely between different types of morphological brain networks (Figure 4, the fourth row and Table S2). Nevertheless, we noted that several regions of the lateral sulcus were consistently identified as hubs for all types of morphological brain networks. Another interesting finding was that several regions (e.g., the left horizontal ramus of the anterior segment of the lateral sulcus and left orbital part of the inferior frontal gyrus) acted as hubs across most participants for the SD networks (maximum probability: 96.8% for degree, 96.0% for efficiency and 83.2% for betweenness), in contrast to the other three types of morphological brain networks (maximum probability: 26.8% ~ 56.3%).

For age-related changes in the hubs, significant results were observed only for the FD and CT networks (Figure 6).

3.3.1 | FD networks

The mean nodal degree ($p = .013$; inflection point: 52; stationary points: 36 and 67) and efficiency ($p = .005$, inflection point: 53; stationary points: 37 and 68) showed a $\sim -$shape curve while the mean nodal betweenness ($p = .005$, inflection point: 55; stationary points: 38 and 71) showed an inverted $\sim -$ shape curve as age increased for the hubs of the FD networks. For the non-hubs, the mean nodal degree ($p = .013$, inflection point: 52; stationary points: 36 and 67) showed an inverted $\sim -$ shape curve as age increased.

3.3.2 | SD networks

The mean nodal efficiency exhibited a U-shape relationship with age for the non-hubs of the SD networks ($p = .003$, peak point: 46).

3.3.3 | CT networks

The mean nodal degree ($p < .001$) and efficiency ($p < .001$) increased linearly while the mean nodal betweenness ($p < .001$) decreased linearly with age for the hubs of the CT networks. For the non-hubs, the mean nodal degree ($p < .001$) and efficiency ($p = .002$) decreased linearly with age.

3.4 | Age-related changes in interregional morphological similarities

We found that the mean morphological similarity matrices across participants in each age bin (Figure S5) were largely comparable regardless of the type of single-subject morphological brain networks as evaluated by both visual check and quantitative spatial correlation analysis (FD networks: $r = .826 \pm .044$; GI networks: $r = .720 \pm .064$; SD networks: $r = .977 \pm .009$; CT networks: $r = .766 \pm .096$) (Figure 7). Nevertheless, significant age-related changes were observed in numerous connections ($p < .05$, FDR corrected; Figures 8 and S6). The age-related changes were mainly characterized by linear changes, and exhibited an anatomical distance-dependent and module-specific patterns.

3.4.1 | FD networks

Significant age-related changes were observed on 1154 morphological connections of the FD networks (linear: 1000, 86.7%; quadratic: 117, 10.1%; cubic: 37, 3.2%).

FIGURE 3 Legend on next page.

3.4.2 | GI networks

Significant age-related changes were observed on 518 morphological connections of the GI networks (linear: 393, 75.9%; quadratic: 101, 19.5%; cubic: 24, 4.6%).

3.4.3 | SD networks

Significant age-related changes were observed on 2125 morphological connections of the SD networks (linear: 1301, 61.2%; quadratic: 644, 30.3%; cubic: 180, 8.5%).

3.4.4 | CT networks

Significant age-related changes were observed on 3588 morphological connections of the CT networks (linear: 2196, 61.2%; quadratic: 1038, 28.9%; cubic: 354, 9.9%).

3.4.5 | Distance-dependent age-related changes in morphological similarities

For all types of morphological brain networks, the age-related changes in interregional morphological similarities preferred connections with short-range anatomical distances ($p < .05$; Figure 9). Further analyses revealed that the preference was mainly observed for the age-related linear and quadratic changes, while the age-related cubic changes preferred connections with long-range anatomical distances (Table S3).

3.4.6 | Module-specific age-related changes in morphological similarities

Module-specific age-related changes in morphological similarities were found for the FD and GI networks. For the FD networks, age-related changes were preferentially susceptible to connections linking the LN and VAN ($p = .003$, FDR corrected), and the LN and FPN ($p = .001$, FDR corrected). For the GI networks, age-related changes were preferentially susceptible to connections linking the LN and VAN ($p = .002$, FDR corrected). When considering different statistical models, we found that only connections that changed linearly with age exhibited the preferential susceptibility for both the FD networks (LN-VAN: $p = .004$; LN-FPN: $p = .002$; VAN-FPN: $p = .003$; all FDR corrected) and GI networks (LN-VAN: $p = .002$, FDR corrected; Figure 10).

3.5 | Cognitive relevance of age-related changes in single-subject morphological brain networks

After controlling for the effects of sex, the Cattell scores were found to significantly correlate with nodal centrality of 52 regions (FD networks: 13; GI networks: 2; SD networks: 17; CT networks: 24; $p < .05$, FDR corrected; Figure S7). The regions mainly concentrated on frontal cortex, and the correlations were mainly characterized by higher nodal centralities for higher Cattell scores. For interregional morphological similarity, massive positive correlations were observed for each type of morphological brain networks (FD networks: 776; GI networks: 262; SD networks: 1186; CT networks: 2027) ($p < .05$, FDR corrected; Figure S8). Of note, negative correlations were also found for many connections of the SD networks. No significant correlations were found between global network measures and the Cattell scores.

After controlling for additional effects of age, only one correlation survived with the Cattell scores: interregional CT similarity between the left superior frontal gyrus and superior part of the precentral sulcus ($r = .173$, $p < .001$) (Figure 11, left).

3.6 | Age-related changes in local morphology

Significant age-related changes in local morphology are shown in Figure S9 ($p < .05$, FDR corrected). In general, the age-related changes were mainly characterized by linear changes, and involved in frontal and temporal cortex regardless of the morphological indices.

3.6.1 | FD

Significant age-related changes (linear: 43, 75.4%; quadratic: 14, 24.6%) were observed on the FD of 57 regions (frontal: 23, 40.4%; temporal: 9, 15.8%).

3.6.2 | GI

Significant age-related changes (linear: 25, 61.0%; quadratic: 14, 34.1%; cubic: 2, 4.9%) were observed on the GI of 41 regions (frontal: 15, 36.6%; temporal: 8, 19.5%).

FIGURE 3 A summary of regions showing age-related changes in nodal centralities. The top-left panel shows the number of regions (y-axis) that exhibit age-related changes at different frequencies (x-axis) among different nodal centrality measures of different types of single-subject morphological brain networks. The top-right panel shows the regions that are mostly affected by age (frequency ≥ 4) with the corresponding age-related trajectories depicted in the bottom panel. Red diamonds denote the peak points of age in the quadratic models, and stars denote stationary points of age in the cubic models. k_i, nodal degree; e_i, nodal efficiency; b_i, nodal betweenness; CT, cortical thickness; FD, fractal dimension; GI, gyrification index; SD, sulcus depth.

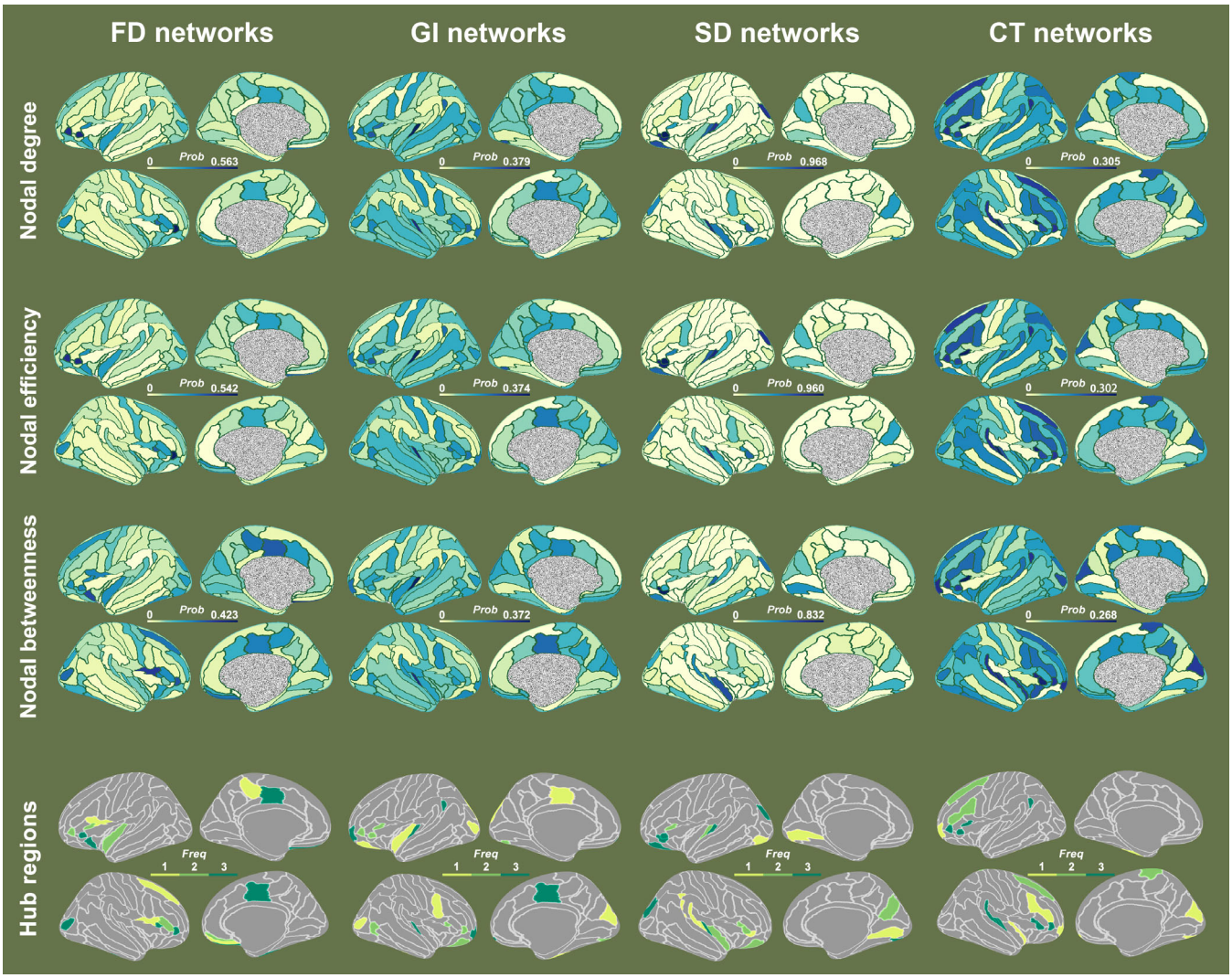

FIGURE 4 Hub probability maps. A hub probability map was calculated for each nodal centrality measure of each type of single-subject morphological brain network as the frequency of a region acting as a hub across all participants (first three rows). Regions with values in the top 10% of the probability were identified as group-level brain hubs, which were further summarized across nodal centrality measures (fourth row). CT, cortical thickness; FD, fractal dimension; GI, gyrification index; SD, sulcus depth.

3.6.3 | SD

Significant age-related changes (linear: 37, 84.1%; quadratic: 7, 15.9%) were observed on the SD of 44 regions (temporal: 11, 25.0%; dividing sulci: 11, 25.0%).

3.6.4 | CT

Significant age-related changes (linear: 51, 71.8%; quadratic: 17, 23.9%; cubic: 2, 4.2%) were observed on the CT of 71 regions (frontal: 27, 38.0%; temporal: 12, 16.9%).

All age-related changes in local morphology are further summarized in Figure S10. We noted several interesting phenomenon: (1) for linear age-related changes, most regions increased with age for the GI (20/25, 80.0%), while decreased with age for the other three indices (FD: 42/43, 97.7%; SD: 36/37, 97.3%; CT: 50/51, 98.0%); (2) quadratic and cubic age-related changes were mainly found in the insula and limbic regions (FD: 6, 42.9%; GI: 5, 31.3%; SD: 5, 71.4%; CT: 11, 55%); and (3) several regions were consistently identified to show age-related changes in multiple morphological indices, such as the right superior frontal gyrus, left posterior-ventral part of cingulate gyrus, triangular part of bilateral inferior frontal gyri and inferior segment of circular sulcus of the bilateral insula.

Out of the regions showing significant age-related changes in their morphology, 125 were significantly correlate with the Cattell scores after controlling for the effects of sex (FD: 51; GI: 29; SD: 42; CT: 71; $p < .05$, FDR corrected; Figure S7). These correlations were mainly characterized by higher morphological values for higher Cattell scores. After controlling for additional effects of age, only two correlations survived with the Cattell scores: CT of the left anterior Heschl's gyrus ($r = .152$, $p < .001$) (Figure 11, middle) and SD of the right

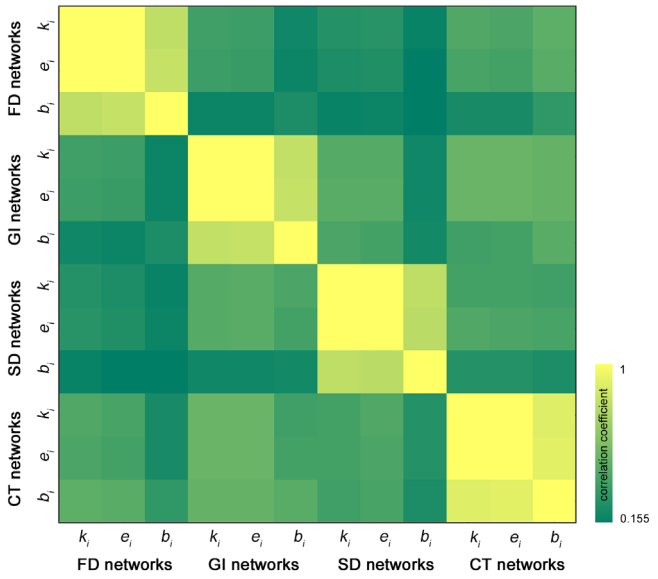

FIGURE 5 Spatial similarities of hub probability maps between different nodal centrality measures of different types of single-subject morphological brain networks. k_i, nodal degree; e_i, nodal efficiency; b_i, nodal betweenness; CT, cortical thickness; FD, fractal dimension; GI, gyrification index; SD, sulcus depth.

horizontal ramus of the anterior segment of the lateral sulcus ($r = .140$, $p < .001$; Figure 11, right).

4 | DISCUSSION

In this study, we investigated age-related changes in single-subject morphological brain networks for healthy adults across 18–88 years old. Compared with regional morphology, much more changes were found in network-level measures, and the changes exhibited characteristic patterns that depended on multiple factors, including the morphological features used for network construction, nodal locations and roles, anatomical distances, and cortical modules.

4.1 | Age related changes in global organization of single-subject morphological brain networks

We found significant age-related changes in global topological organization only for the CT networks. Specifically, clustering coefficient and local efficiency declined linearly with the increase of age. Both clustering coefficient and local efficiency are measures of functional segregation, that is, the ability for specialized processing occurring among densely interconnected brain regions. Thus, our findings indicate continually decreased functional segregation of the CT networks during the age-related process. This is consistent with previous studies of single-subject morphological brain networks based on gray matter volume, which found a negative correlation for clustering coefficient and local efficiency with age (Kong et al., 2015; Shigemoto et al., 2023). However, using the same method as this work, a recent study found that clustering coefficient of CT networks showed an inverted U-shaped age-related trajectory (Wang et al., 2022). This discrepancy may be due to differences between the current study and previous one in the statistical model used (linear, quadratic, and cubic vs. quadratic) and/or in the data homogeneity with respect to site (single vs. multiple) and field strength (3 T vs. 1.5/3 T).

Beyond age-related linear decline in functional segregation, we found that functional integration as indexed by characteristic path length and global efficiency exhibited cubic age-related trajectory. Functional integration is the ability of the brain to rapidly integrate specialized information from distributed brain regions. Thus, our results suggest a fluctuant change in functional integration of the CT networks across the adult lifespan: decreasing between ages 18 and 41, then increasing between ages 41 and 57, and finally decreasing until age 88. Notably, the cubic age-related changes are first reported since none of previous studies utilized the cubic model to examine the age-related changes in single-subject morphological brain networks (Kong et al., 2015; Shigemoto et al., 2023; Wang et al., 2022). Moreover, findings from the previous studies were different or even opposite possibly due to different statistical models and network construction methods. Accordingly, more studies are needed in the future to systematically explore age-related changes in single-subject morphological brain networks.

4.2 | Age-related changes in local organization of single-subject morphological brain networks

We found significant age-related changes in multiple brain regions that were mainly located in frontal regions. This was also the case for our findings of age-related changes in local morphology. Previous studies found that structural and metabolic changes with age predominantly occurred in (pre)frontal cortices (Alexander et al., 2006; Allen et al., 2005; Jernigan et al., 2001; Shaw et al., 1984; Sowell et al., 2003; Ziegler et al., 2012). Similar findings were observed for brain network studies of development and aging (Shah et al., 2018; Váša et al., 2018; Zhao et al., 2015). Thus, our results are consistent with previous studies, which provide new evidence from single-subject morphological brain networks for the frontal susceptibility to age. The frontal lobe is engaged in a variety of higher cognitive functions, such as working memory, executive function, and problem solving. Thus, the frontal susceptibility to age may explain the reason for cognitive decline in elderly populations (Park et al., 2003). In addition, frontal regions have been found to be disproportionately implicated in different brain diseases. For example, patients with Alzheimer's disease patients were found to show reduced nodal efficiency predominantly located in frontal regions (Lo et al., 2010). This implies the caution to avoid possible confounding effects from normal age-related changes in frontal alterations in age-related brain diseases.

In addition to the frontal susceptibility, we found that age-related changes were mainly observed for hub regions, which exhibited differential age-related trajectories from non-hubs. The existence of highly

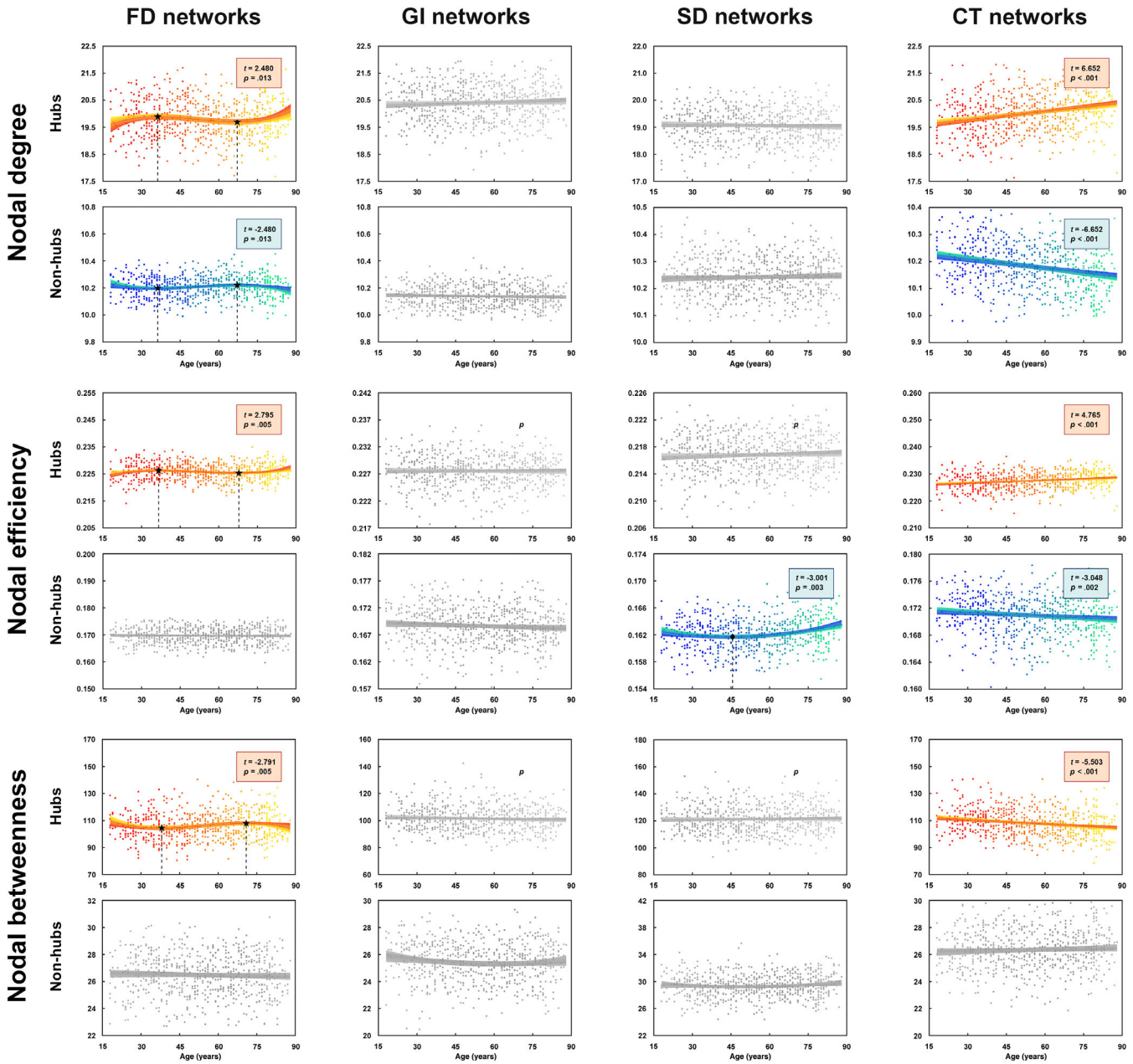

FIGURE 6 Age-related changes in hubs and non-hubs. Colored scatterplots indicate significant age-related changes. Black diamond denotes the peak points of age in the quadratic model, and black stars denote stationary points of age in the cubic models. CT, cortical thickness; FD, fractal dimension; GI, gyrification index; SD, sulcus depth.

connected hubs is a universal finding for human brain networks (van den Heuvel & Sporns, 2013). Hubs play a critically important role in enabling efficient neuronal signaling and communication in the brain (van den Heuvel et al., 2012), but meanwhile they are associated with high wiring costs and metabolic demands (Liang et al., 2013; Tomasi et al., 2013; van den Heuvel et al., 2012), which render them points of vulnerability in brain disorders (Crossley et al., 2014). In the domain of development and aging, hubs are also found to be the main brain regions to manifest age-related changes in structural and functional brain networks (Betzel et al., 2014; Cao et al., 2014; Zhao et al., 2019). Consistent with these findings, our results further support the vulnerability of hubs to age-related changes. Compared with non-hubs, hubs are more densely interconnected, forming a rich-club organization (van den Heuvel & Sporns, 2011). Previous studies of structural brain networks found that connections of hubs were disproportionately influenced by development and aging (Baker et al., 2015; Li et al., 2023). In parallel, a recent study found that genes played a preferential role in shaping the connections between hubs (Arnatkeviciute et al., 2021). We thus speculate that genes may be an important factor in accounting for the vulnerability of hubs to age-related changes. It should be noted that how to define hubs is an ongoing research topic (Wang et al., 2018), and different types of hubs were found to exhibit distinct age-related trajectories of their connections (Zhang et al., 2021). Accordingly, more studies are

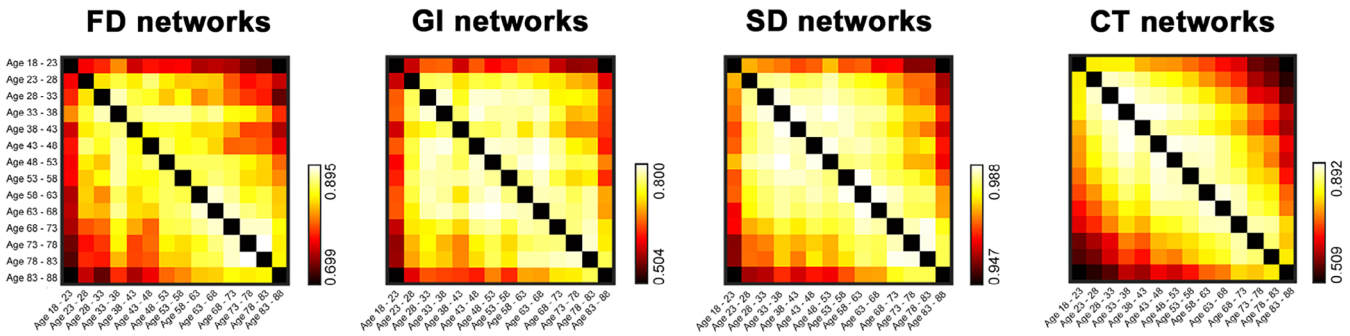

FIGURE 7 Spatial similarities of mean morphological similarity matrices between different age bins. CT, cortical thickness; FD, fractal dimension; GI, gyrification index; SD, sulcus depth.

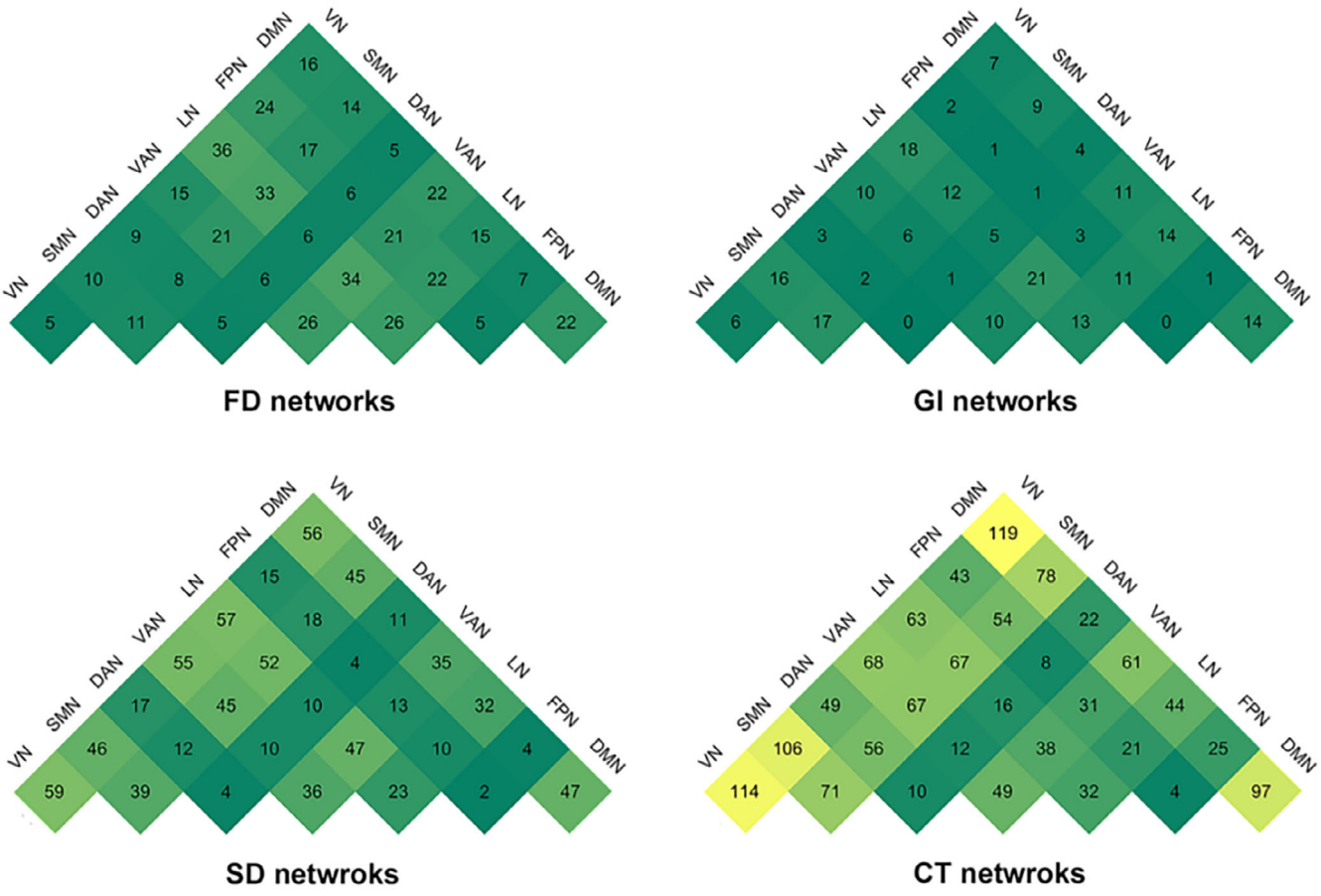

FIGURE 8 The number of morphological connections showing age-related changes within and between modules. CT, cortical thickness; DAN, dorsal attention network; DMN, default mode network; FD, fractal dimension; FPN, frontoparietal network; GI, gyrification index; LN, limbic network; SD, sulcus depth; SMN, somatomotor network; VAN, ventral attention network; VN, visual network.

required in the future to deepen our understanding of the roles and categories of hubs and how hubs emerge, develop, mature and degenerate through the whole lifespan. Interestingly, we found that several regions were consistently identified as hubs in the SD networks for most participants, indicating that the key roles of these regions are stable across the adult lifespan. In the future, it is important to explore whether the roles of this specific set of regions are altered in neurodevelopmental and neurodegenerative disorders.

4.3 | Age-related changes in interregional similarity of single-subject morphological brain networks

Numerous interregional morphological similarities were identified to show significant age-related changes, which were mainly involved in short-range connections regardless of the type of morphological brain networks. Short-range connections between nearby regions are thought to predominate in brain networks, which are responsible for

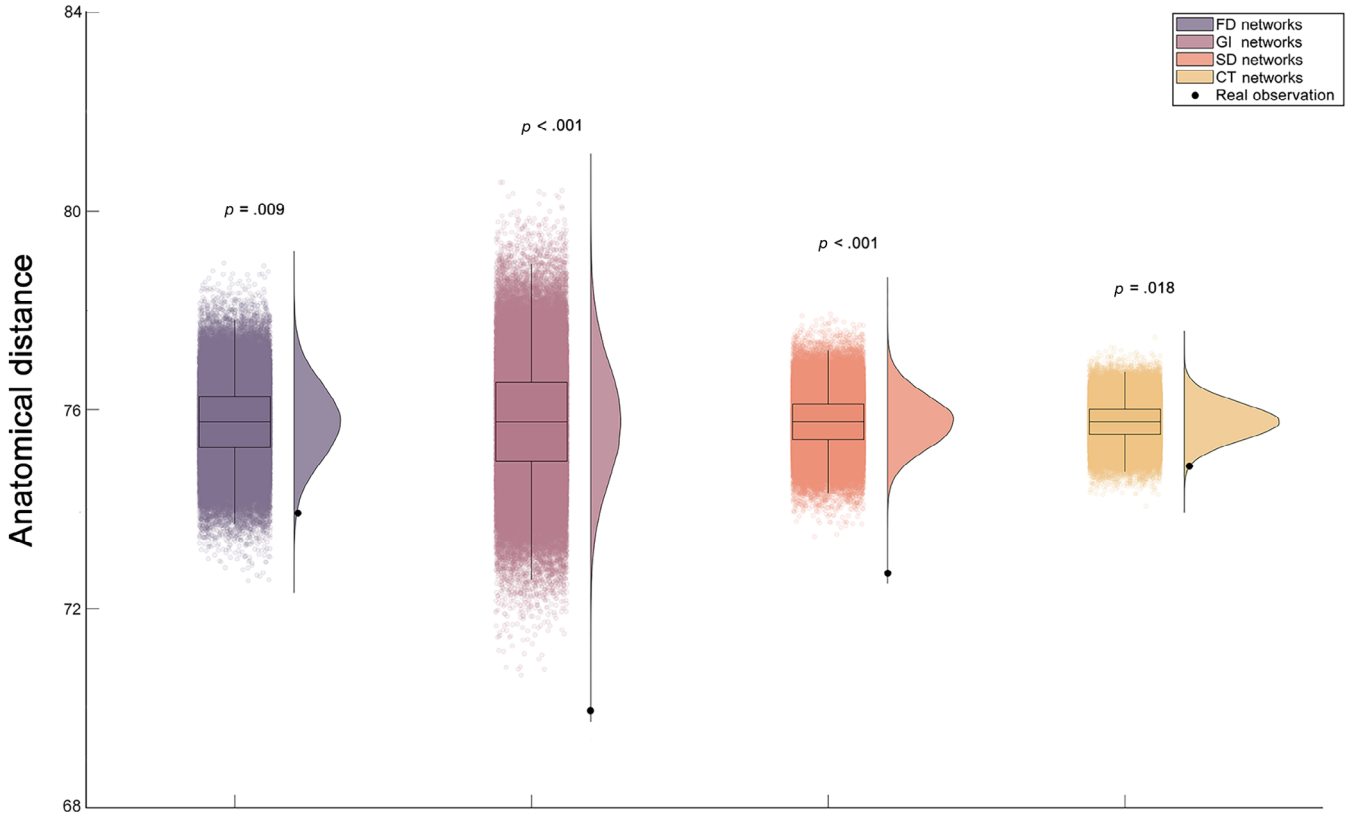

FIGURE 9 Distance-dependent age-related changes in interregional morphological similarities. For all types of single-subject morphological brain networks, the morphological similarities showing significant age-related changes were mainly involved in connections with short-range anatomical distances. CT, cortical thickness; FD, fractal dimension; GI, gyrification index; SD, sulcus depth.

specialized or modular information processing (Zhang, 2011). Thus, our findings suggest changes in the extent of functional segregation as general and major age-related changes in single-subject morphological brain networks. This is consistent with previous studies reporting that age-related changes are associated with altered modularity of functional brain networks (Onoda & Yamaguchi, 2013; Song et al., 2014). For brain development, a previous structural brain network study of preterm-born and full-term neonates found that edge strength of short-range exhibited faster developmental rates than that of long-range connections (Zhao et al., 2019, p. 201). These findings suggest important roles of short-range connections in brain development and aging. Anatomical distance is an important determinant of the formation of brain network topology (Vértes et al., 2012), which is conceptualized as an economic trade-off between minimizing wiring costs through reducing connection distance and maximizing efficiency by adding expensive but beneficial long-range connections (Bullmore & Sporns, 2012). However, compared with well-studied long-range connections, the roles of short-range connections are worse understood in the context of brain development and aging, which, however, are recently argued to be as neuroscientifically and clinically important as the long-range connections (Ouyang et al., 2017). It should be noted that the preference for short-range connections was mainly due to age-related linear and quadratic changes in interregional morphological similarity. For age-related cubic changes, a preference for long-range connections was observed. These findings suggest differential roles of anatomical distance in morphological connections showing different age-related trajectories. More insights into these interesting findings can be obtained by examining other types of brain networks with respect to the relationship between anatomical distance and age-related trajectories.

In addition to the anatomical distance-dependent age-related changes, we characterized the distribution of morphological similarities showing age-related changes in the context of cerebral modular architecture. We found that the morphological similarities showing age-related changes were selectively involved in connections between specific pairs of modules (LN-VAN, LN-FPN and VAN-FPN). The LN is central for processing and regulating emotion (Dalgleish, 2004); the FPN is mainly dedicated to cognitive control (Zanto & Gazzaley, 2013); the VAN interrupts and resets attention to behaviorally salient stimuli (Corbetta et al., 2008). These processes are not isolated but rather interact with each other in a complicated manner. For example, there is a large amount of evidence for the key roles of attentional orienting and cognitive control in emotion regulation (Viviani, 2013). In particular, a recent study found that age-related loss of inter-network functional connectivity was primarily driven by functional connectivity reductions in frontal and parietal association cortices (Hrybouski et al., 2021). Moreover, age-related changes in between-network functional connectivity of the FPN were found to

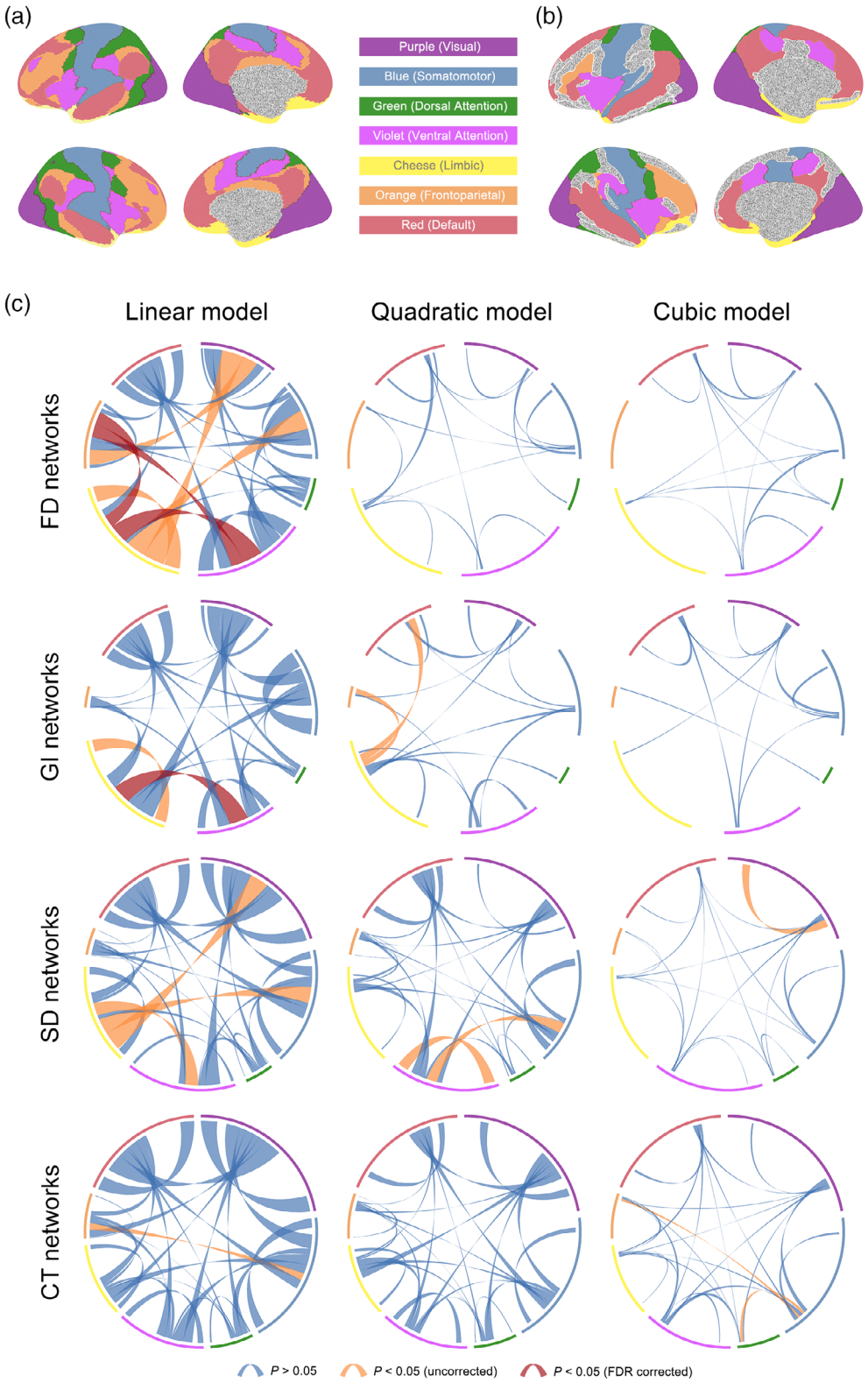

FIGURE 10 Module-specific age-related changes in interregional morphological similarities. (a) Functional modules from Yeo's 7-networks atlas. (b) Assignation of regions in the Destrieux atlas to the functional modules from Yeo's 7-networks atlas. (c) Susceptibility of age-related changes to connections liking specific pairs of functional modules. Age-related linear changes in interregional morphological similarities were susceptible to connections between the LN and VAN, LN and FPN, and VAN and FPN for the FD networks, and connections between the LN and VAN for the GI networks. CT, cortical thickness; FD, fractal dimension; GI, gyrification index; SD, sulcus depth.

predict cognitive performance (Grady et al., 2016), and the FPN mediated the associations of other networks with cognition (E. E. Shaw et al., 2015). Based on these findings, we speculate that the preference of age-related changes for the connections between specific sets of functional systems, in particular those linking the FPN, may be responsible for individual variation in cognition.

4.4 | Distinct age-related changes in different types of single-subject morphological brain networks

We found that different types of single-subject morphological brain networks exhibited distinct patterns of age-related changes in their topological organization at multiple levels. The distinction was

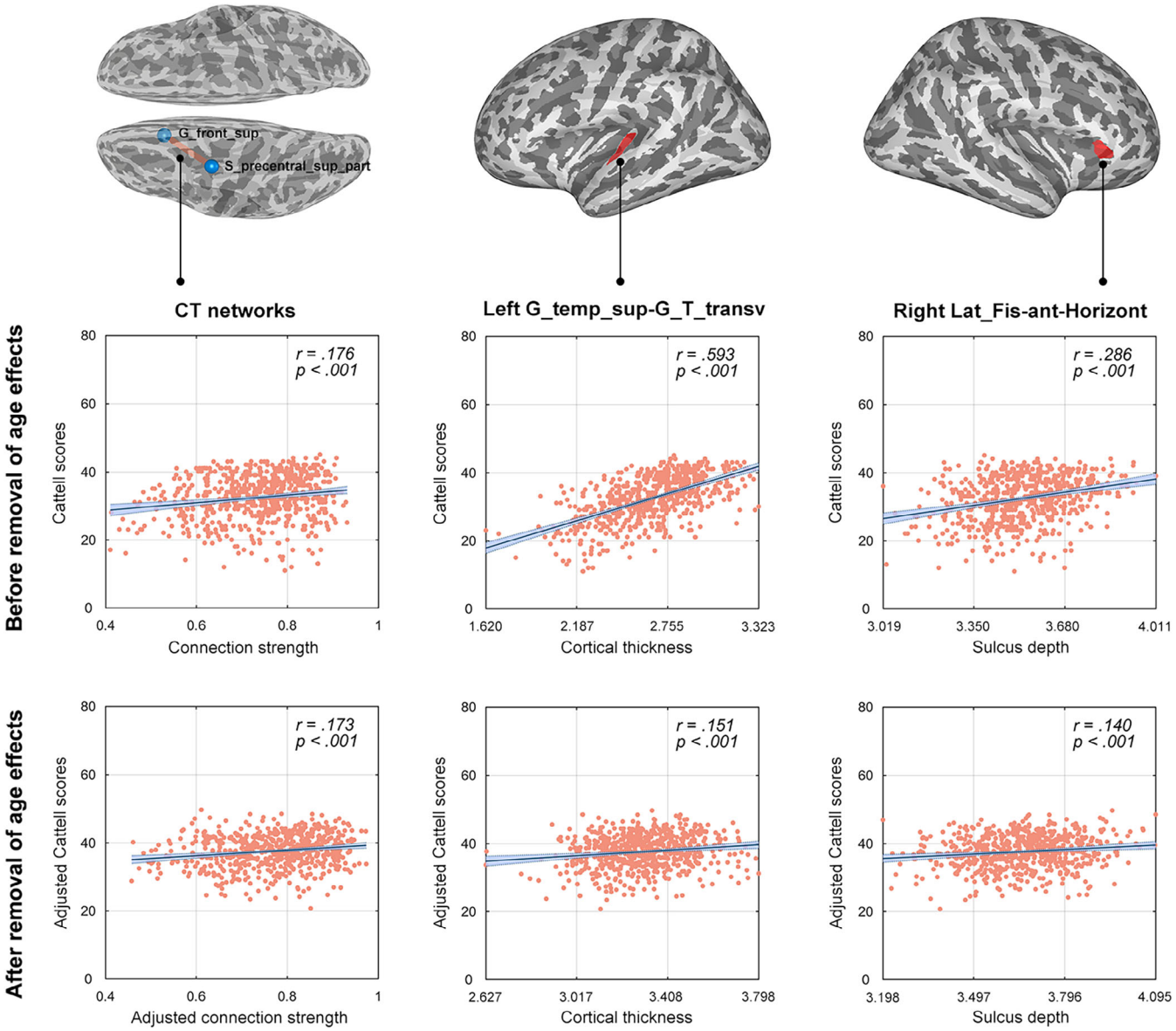

FIGURE 11 Relationships of the Cattell scores with interregional morphological similarity and local morphology. Before and after controlling for effects of age, individual Cattell scores were consistently found to show positive correlations with interregional CT similarity between the left superior frontal gyrus and superior part of the precentral sulcus, cortical thickness of the left anterior transverse temporal gyrus, and sulcus depth of the right horizontal ramus of the anterior segment of the lateral sulcus. CT, cortical thickness.

embodied in not only the presence or absence of age-related changes but also the trajectories when age-related changes were commonly observed. This is as expected since different morphological features possess distinct cellular mechanisms, genetic origins and/or developmental/aging trajectories. For example, CT and GI, which are thought to separately capture the laminar structure (Adler-Wagstyl & Lerch, 2018) and complexity of cerebral cortex (Yotter et al., 2011), were previously reported to show strongest age-related changes in frontal and parietal regions, respectively, across adult lifespan (Hogstrom et al., 2013). Nevertheless, it seems that the distinct patterns cannot be explained by age-related differences in the morphological features themselves since poor correspondences were found in the regions with age-related changes between local morphology and nodal centralities of single-subject morphological brain networks. It is particularly noteworthy that the age-related changes appear predominantly concentrated on the CT networks, in which global and more regional and connectional changes were observed. These findings suggest that CT single-subject morphological brain networks are more vulnerable to age-related changes. However, our previous study found that CT single-subject morphological brain networks performed worse than the other three types of networks with respect to test–retest reliability (Li et al., 2021). Thus, more studies are warranted to validate our results.

4.5 | Linear changes dominate age-related changes in single-subject morphological brain networks

In this study, we employed linear, quadratic, and cubic models to explore age-related trajectories of single-subject morphological brain networks. We found that the age-related changes in nodal centrality measures and interregional morphological similarities of the morphological brain networks as well as local morphology were all dominated by linear changes with advancing age. Previous studies on healthy adults found that the total gray matter volume decreases linearly with age (Allen et al., 2005; Ge et al., 2002; Good et al., 2001). The global linear decrease may be the reason why gray matter volume of almost all regions of the cerebral cortex exhibited negative correlations with age (Ziegler et al., 2012), and might also be a potential source of the linear dominated age-related changes in morphological brain networks observed in this study. Nevertheless, we noted nonlinear age-related changes in the insula and several limbic regions, such as the cingulate gyrus and parahippocampal gyrus. This is consistent with previous studies showing nonlinear effects of age on CT in the insula and cingulate gyrus (Hogstrom et al., 2013), gray matter volume in the parahippocampal gyrus (Curiati et al., 2009), and functional connectivity of the insula (Zuo et al., 2010). In the future, more comprehensive analyses of these nonlinear age-related changes are required by integrating different approaches and measures derived from multimodal MRI data.

4.6 | Single-subject morphological brain networks account for interindividual differences in cognition

We found that individual Cattell scores were correlated with numerous nodal centralities and interregional morphological similarities of the single-subject morphological brain networks that exhibited significant age-related changes. Our previous study found that single-subject cortical morphological brain networks could explain interindividual variance in behaviors and cognition, and predict individual behavioral and cognitive outcomes (Li, Li, et al., 2022). Using a different method to construct single-subject morphological brain networks, a recent work found that individual general intelligence can be predicted by nodal degree of single-subject morphological brain networks (Seidlitz et al., 2018). These findings collectively indicate that single-subject morphological brain networks are functionally relevant, and provide a promising means to reveal neural substrates of behaviors and cognition. A deeper understanding of the functional relevance of single-subject morphological brain networks may benefit from future studies that explore their plastic changes associated with skill learning and expertise. In addition to the phenotypic associations, single-subject morphological brain networks were further demonstrated to be related to brain-wide gene expression, and cytoarchitecture and chemoarchitecture of the brain (Li, Li, et al., 2022; Seidlitz et al., 2018), suggesting their neurobiological substrates. Interestingly, we found that after controlling for the effects of age, the Cattell scores were still correlated to interregional CT similarity between the left superior frontal gyrus and superior part of the precentral sulcus. This finding suggests a mediating role of the particular morphological connection in the relationship between age and cognition. Thus, an interesting topic in the future is to test whether age-related decline in cognition can be postponed through neuromodulation targeted at brain structures involved in this connection.

4.7 | Limitations, methodological considerations, and future directions

First, four morphological indices were calculated with the CAT12 toolbox to construct single-subject morphological brain networks. It is not clear whether similar age-related changes could be found when other methods or toolboxes are used to estimate the morphological indices. Second, this study examined age-related changes in most commonly used network measures. Besides these measures, future studies are warranted to explore how other organizational principles of single-subject morphological brain networks (e.g., modular composition and rich-club architecture) change with the increase of age. Third, although we found numerous age-related changes in single-subject morphological brain networks, the R^2 of the statistical models were relatively small. This implies that there may exist other factors exerting influence on single-subject morphological brain networks (e.g., experience-based plasticity and environmental contributions). How these factors interact with age to collectively influence single-subject morphological brain networks deserves further study. Fourth, previous studies found that regional size affected to some extent nodal centrality measures of single-subject morphological brain networks (Li et al., 2021; Seidlitz et al., 2018). Thus, it is important for future studies to examine age-related changes in single-subject morphological brain networks by using approximately equally-sized parcellation of brain regions. Fifth, this study examined age-related changes in single-subject morphological brain networks. By combination with other MRI modalities, it is important to examine the extent to which our findings are similar or dissimilar to those revealed by functional and structural brain networks. Finally, our findings of age-related changes in single-subject morphological brain networks have important clinical implications for neurodevelopmental and neurodegenerative disorders, which are increasingly demonstrated to be characterized by deviation from normal developmental and aging trajectories of brain network topology (e.g., Li, Huang, et al., 2022). Particularly, a previous study analyzed structural MRI data from 484 healthy participants, and found a newtork of mainly higher-order regions that linked development, aging, and vulnerability to disease (Douaud et al., 2014). Thus, it is an important topic for future studies to explore atypical development and aging of single-subject cortical morphological brain networks in various neurodevelopmental and neurodegenerative disorders.

5 | CONCLUSIONS

In conclusion, this study systematically examined age-related changes in single-subject morphological brain networks across the adult

lifespan, and found that the changes were mainly embodied in CT networks, characterized by linear changes, concentrated on frontal regions and hubs, involved in short-range connections, and susceptible to connections between the LN, VAN, and FPN. Compared with regional morphology, network-level analysis better characterized age-related changes in the brain. These findings are helpful for understanding interindividual differences in behaviors and cognition.

AUTHOR CONTRIBUTIONS

Jinhui Wang designed the study. Jingxuan Ruan, Ningkai Wang, Junle Li and Jing Wang analyzed data. Jingxuan Ruan and Ningkai Wang wrote the manuscript; Jinhui Wang, Jing Wang, Yating Lv and Qihong Zou revised the manuscript.

ACKNOWLEDGMENTS

This work was supported by the National Natural Science Foundation of China (No. 81922036), Key Realm R&D Program of Guangdong Province (No. 2019B030335001), Key Realm R&D Program of Guangzhou (No. 202007030005) and National Social Science Foundation of China (No. 20&ZD296).

CONFLICT OF INTEREST STATEMENT

The authors declare no competing interests.

DATA AVAILABILITY STATEMENT

The data that support the findings of this study are openly available in Cam-CAN collaborative research project at http://www.mrc-cbu.cam.ac.uk/datasets/camcan/.

ORCID

Jingxuan Ruan https://orcid.org/0000-0003-4900-3184
Ningkai Wang https://orcid.org/0000-0002-2363-9021
Qihong Zou https://orcid.org/0000-0001-8732-6633

REFERENCES

Achard, S., & Bullmore, E. (2007). Efficiency and cost of economical brain functional networks. *PLoS Computational Biology*, *3*(2), e17. https://doi.org/10.1371/journal.pcbi.0030017

Adler-Wagstyl, K., & Lerch, J. (2018). Cortical thickness. *Neuromethods*, *136*, 35–49. https://doi.org/10.1007/978-1-4939-7647-8_3

Akaike, H. (1974). A new look at the statistical model identification. *IEEE Transactions on Automatic Control*, *19*(6), 716–723. https://doi.org/10.1109/TAC.1974.1100705

Alexander, G. E., Chen, K., Merkley, T. L., Reiman, E. M., Caselli, R. J., Aschenbrenner, M., Santerre-Lemmon, L., Lewis, D. J., Pietrini, P., Teipel, S. J., Hampel, H., Rapoport, S. I., & Moeller, J. R. (2006). Regional network of magnetic resonance imaging gray matter volume in healthy aging. *Neuroreport*, *17*(10), 951–956. https://doi.org/10.1097/01.wnr.0000220135.16844.b6

Allen, J. S., Bruss, J., Brown, C. K., & Damasio, H. (2005). Normal neuroanatomical variation due to age: The major lobes and a parcellation of the temporal region. *Neurobiology of Aging*, *26*(9), 1245–1260. https://doi.org/10.1016/j.neurobiolaging.2005.05.023

Arnatkeviciute, A., Fulcher, B. D., Oldham, S., Tiego, J., Paquola, C., Gerring, Z., Aquino, K., Hawi, Z., Johnson, B., Ball, G., Klein, M., Deco, G., Franke, B., Bellgrove, M. A., & Fornito, A. (2021). Genetic influences on hub connectivity of the human connectome. *Nature Communications*, *12*(1), 4237. https://doi.org/10.1038/s41467-021-24306-2

Ay, U., Kizilates-Evin, G., Bayram, A., Kurt, E., & Demiralp, T. (2022). Comparison of FreeSurfer and CAT12 software in parcel-based cortical thickness calculations. *Brain Topography*, *35*(5–6), 572–582. https://doi.org/10.1007/s10548-022-00919-8

Baker, S. T. E., Lubman, D. I., Yucel, M., Allen, N. B., Whittle, S., Fulcher, B. D., Zalesky, A., & Fornito, A. (2015). Developmental changes in brain network hub connectivity in late adolescence. *Journal of Neuroscience*, *35*(24), 9078–9087. https://doi.org/10.1523/JNEUROSCI.5043-14.2015

Bassett, D. S., Bullmore, E., Verchinski, B. A., Mattay, V. S., Weinberger, D. R., & Meyer-Lindenberg, A. (2008). Hierarchical organization of human cortical networks in health and schizophrenia. *The Journal of Neuroscience*, *28*(37), 9239–9248. https://doi.org/10.1523/JNEUROSCI.1929-08.2008

Betzel, R. F., Byrge, L., He, Y., Goñi, J., Zuo, X.-N., & Sporns, O. (2014). Changes in structural and functional connectivity among resting-state networks across the human lifespan. *NeuroImage*, *102*, 345–357. https://doi.org/10.1016/j.neuroimage.2014.07.067

Bullmore, E., & Sporns, O. (2009). Complex brain networks: Graph theoretical analysis of structural and functional systems. *Nature Reviews Neuroscience*, *10*(3), 186–198. https://doi.org/10.1038/nrn2575

Bullmore, E., & Sporns, O. (2012). The economy of brain network organization. *Nature Reviews Neuroscience*, *13*(5), 336–349. https://doi.org/10.1038/nrn3214

Cam-CAN, Shafto, M. A., Tyler, L. K., Dixon, M., Taylor, J. R., Rowe, J. B., Cusack, R., Calder, A. J., Marslen-Wilson, W. D., Duncan, J., Dalgleish, T., Henson, R. N., Brayne, C., & Matthews, F. E. (2014). The cambridge centre for ageing and neuroscience (Cam-CAN) study protocol: A cross-sectional, lifespan, multidisciplinary examination of healthy cognitive ageing. *BMC Neurology*, *14*(1), 204. https://doi.org/10.1186/s12883-014-0204-1

Cao, M., Huang, H., & He, Y. (2017). Developmental connectomics from infancy through early childhood. *Trends in Neurosciences*, *40*(8), 494–506. https://doi.org/10.1016/j.tins.2017.06.003

Cao, M., Wang, J.-H., Dai, Z.-J., Cao, X.-Y., Jiang, L.-L., Fan, F.-M., Song, X.-W., Xia, M.-R., Shu, N., Dong, Q., Milham, M. P., Castellanos, F. X., Zuo, X.-N., & He, Y. (2014). Topological organization of the human brain functional connectome across the lifespan. *Developmental Cognitive Neuroscience*, *7*, 76–93. https://doi.org/10.1016/j.dcn.2013.11.004

Chen, Z. J., He, Y., Rosa-Neto, P., Gong, G., & Evans, A. C. (2011). Age-related alterations in the modular organization of structural cortical network by using cortical thickness from MRI. *NeuroImage*, *56*(1), 235–245. https://doi.org/10.1016/j.neuroimage.2011.01.010

Corbetta, M., Patel, G., & Shulman, G. L. (2008). The reorienting system of the human brain: From environment to theory of mind. *Neuron*, *58*(3), 306–324. https://doi.org/10.1016/j.neuron.2008.04.017

Crossley, N. A., Mechelli, A., Scott, J., Carletti, F., Fox, P. T., McGuire, P., & Bullmore, E. T. (2014). The hubs of the human connectome are generally implicated in the anatomy of brain disorders. *Brain*, *137*(8), 2382–2395. https://doi.org/10.1093/brain/awu132

Curiati, P. K., Tamashiro, J. H., Squarzoni, P., Duran, F. L. S., Santos, L. C., Wajngarten, M., Leite, C. C., Vallada, H., Menezes, P. R., Scazufca, M., Busatto, G. F., & Alves, T. C. T. F. (2009). Brain structural variability due to aging and gender in cognitively healthy elders: Results from the São Paulo ageing and health study. *American Journal of Neuroradiology*, *30*(10), 1850–1856. https://doi.org/10.3174/ajnr.A1727

Dalgleish, T. (2004). The emotional brain. *Nature Reviews Neuroscience*, *5*(7), 583–589. https://doi.org/10.1038/nrn1432

Destrieux, C., Fischl, B., Dale, A., & Halgren, E. (2010). Automatic parcellation of human cortical gyri and sulci using standard anatomical nomenclature. *NeuroImage*, *53*(1), 1–15. https://doi.org/10.1016/j.neuroimage.2010.06.010

Douaud, G., Groves, A. R., Tamnes, C. K., Westlye, L. T., Duff, E. P., Engvig, A., Walhovd, K. B., James, A., Gass, A., Monsch, A. U., Matthews, P. M., Fjell, A. M., Smith, S. M., & Johansen-Berg, H. (2014). A common brain network links development, aging, and vulnerability to disease. *Proceedings of the National Academy of Sciences*, *111*(49), 17648–17653. https://doi.org/10.1073/pnas.1410378111

Fenchel, D., Dimitrova, R., Seidlitz, J., Robinson, E. C., Batalle, D., Hutter, J., Christiaens, D., Pietsch, M., Brandon, J., Hughes, E. J., Allsop, J., O'Keeffe, C., Price, A. N., Cordero-Grande, L., Schuh, A., Makropoulos, A., Passerat-Palmbach, J., Bozek, J., Rueckert, D., … O'Muircheartaigh, J. (2020). Development of microstructural and morphological cortical profiles in the neonatal brain. *Cerebral Cortex*, *30*(11), 5767–5779. https://doi.org/10.1093/cercor/bhaa150

Galdi, P., Blesa, M., Stoye, D. Q., Sullivan, G., Lamb, G. J., Quigley, A. J., Thrippleton, M. J., Bastin, M. E., & Boardman, J. P. (2020). Neonatal morphometric similarity mapping for predicting brain age and characterizing neuroanatomic variation associated with preterm birth. *NeuroImage: Clinical*, *25*, 102195. https://doi.org/10.1016/j.nicl.2020.102195

Ge, Y., Grossman, R. I., Babb, J. S., Rabin, M. L., Mannon, L. J., & Kolson, D. L. (2002). Age-related total gray matter and white matter changes in normal adult brain. Part I: Volumetric MR imaging analysis. *American Journal of Neuroradiology*, *23*(8), 1327–1333. http://www.ajnr.org/content/23/8/1327

Good, C. D., Johnsrude, I. S., Ashburner, J., Henson, R. N. A., Friston, K. J., & Frackowiak, R. S. J. (2001). A voxel-based morphometric study of ageing in 465 Normal adult human brains. *NeuroImage*, *14*(1), 21–36. https://doi.org/10.1006/nimg.2001.0786

Grady, C., Sarraf, S., Saverino, C., & Campbell, K. (2016). Age differences in the functional interactions among the default, frontoparietal control, and dorsal attention networks. *Neurobiology of Aging*, *41*, 159–172. https://doi.org/10.1016/j.neurobiolaging.2016.02.020

He, Y., Chen, Z. J., & Evans, A. C. (2007). Small-world anatomical networks in the human brain revealed by cortical thickness from MRI. *Cerebral Cortex*, *17*(10), 2407–2419. https://doi.org/10.1093/cercor/bhl149

Hogstrom, L. J., Westlye, L. T., Walhovd, K. B., & Fjell, A. M. (2013). The structure of the cerebral cortex across adult life: Age-related patterns of surface area, thickness, and gyrification. *Cerebral Cortex*, *23*(11), 2521–2530. https://doi.org/10.1093/cercor/bhs231

Hrybouski, S., Cribben, I., McGonigle, J., Olsen, F., Carter, R., Seres, P., Madan, C. R., & Malykhin, N. V. (2021). Investigating the effects of healthy cognitive aging on brain functional connectivity using 4.7 T resting-state functional magnetic resonance imaging. *Brain Structure and Function*, *226*(4), 1067–1098. https://doi.org/10.1007/s00429-021-02226-7

Hurvich, C. M., & Tsai, C. L. (1989). Regression and time series model selection in small samples. *Biometrika*, *76*(2), 297–307. https://doi.org/10.1093/biomet/76.2.297

Jernigan, T. L., Archibald, S. L., Fennema-Notestine, C., Gamst, A. C., Stout, J. C., Bonner, J., & Hesselink, J. R. (2001). Effects of age on tissues and regions of the cerebrum and cerebellum. *Neurobiology of Aging*, *22*(4), 581–594. https://doi.org/10.1016/S0197-4580(01)00217-2

Kievit, R. A., Davis, S. W., Mitchell, D. J., Taylor, J. R., Duncan, J., Cam-CAN Research team, Tyler, L. K., Brayne, C., Bullmore, E., Calder, A., Cusack, R., Dalgleish, T., Matthews, F., Marslen-Wilson, W., Rowe, J., Shafto, M., Campbell, K., Cheung, T., Geerligs, L., … Henson, R. N. A. (2014). Distinct aspects of frontal lobe structure mediate age-related differences in fluid intelligence and multitasking. *Nature Communications*, *5*(1), 5658. https://doi.org/10.1038/ncomms6658

Kong, X., Liu, Z., Huang, L., Wang, X., Yang, Z., Zhou, G., Zhen, Z., & Liu, J. (2015). Mapping individual brain networks using statistical similarity in regional morphology from MRI. *PLoS One*, *10*(11), e0141840. https://doi.org/10.1371/journal.pone.0141840

Li, J., Huang, M., Pan, F., Li, Z., Shen, Z., Jin, K., Zhao, H., Lu, S., Shang, D., Xu, Y., & Wang, J. (2022). Aberrant development of cross-frequency multiplex functional connectome in first-episode, drug-naive major depressive disorder and schizophrenia. *Brain Connectivity*, *12*(6), 538–548. https://doi.org/10.1089/brain.2021.0088

Li, W., Yang, C., Shi, F., Wu, S., Wang, Q., Nie, Y., & Zhang, X. (2017). Construction of individual morphological brain networks with multiple morphometric features. *Frontiers in Neuroanatomy*, *11*, 34. https://doi.org/10.3389/fnana.2017.00034

Li, X., Salami, A., & Persson, J. (2023). Hub architecture of the human structural connectome: Links to aging and processing speed. *Neuroscience*, *278*, 120270. https://doi.org/10.1101/2023.01.28.525980

Li, Y., Wang, N., Wang, H., Lv, Y., Zou, Q., & Wang, J. (2021). Surface-based single-subject morphological brain networks: Effects of morphological index, brain parcellation and similarity measure, sample size-varying stability and test-retest reliability. *NeuroImage*, *235*, 118018. https://doi.org/10.1016/j.neuroimage.2021.118018

Li, Z., Li, J., Wang, N., Lv, Y., Zou, Q., & Wang, J. (2022). Cortical morphological brain networks: Phenotypic associations and microbiological substrates. https://doi.org/10.2139/ssrn.4094329

Liang, X., Zou, Q., He, Y., & Yang, Y. (2013). Coupling of functional connectivity and regional cerebral blood flow reveals a physiological basis for network hubs of the human brain. *Proceedings of the National Academy of Sciences*, *110*(5), 1929–1934. https://doi.org/10.1073/pnas.1214900110

Liao, X., Vasilakos, A. V., & He, Y. (2017). Small-world human brain networks: Perspectives and challenges. *Neuroscience & Biobehavioral Reviews*, *77*, 286–300. https://doi.org/10.1016/j.neubiorev.2017.03.018

Lo, C.-Y., Wang, P.-N., Chou, K.-H., Wang, J., He, Y., & Lin, C.-P. (2010). Diffusion tensor tractography reveals abnormal topological organization in structural cortical networks in Alzheimer's disease. *The Journal of Neuroscience*, *30*(50), 16876–16885. https://doi.org/10.1523/JNEUROSCI.4136-10.2010

Luders, E., Thompson, P. M., Narr, K. L., Toga, A. W., Jancke, L., & Gaser, C. (2006). A curvature-based approach to estimate local gyrification on the cortical surface. *NeuroImage*, *29*(4), 1224–1230. https://doi.org/10.1016/j.neuroimage.2005.08.049

Lv, Y., Wei, W., Han, X., Song, Y., Han, Y., Zhou, C., Zhou, D., Zhang, F., Wu, X., Liu, J., Zhao, L., Zhang, C., Wang, N., & Wang, J. (2021). Multiparametric and multilevel characterization of morphological alterations in patients with transient ischemic attack. *Human Brain Mapping*, *42*(7), 2045–2060. https://doi.org/10.1002/hbm.25344

Madden, D. J., Spaniol, J., Costello, M. C., Bucur, B., White, L. E., Cabeza, R., Davis, S. W., Dennis, N. A., Provenzale, J. M., & Huettel, S. A. (2008). Cerebral white matter integrity mediates adult age differences in cognitive performance. *Journal of Cognitive Neuroscience*, *21*(2), 289–302. https://doi.org/10.1162/jocn.2009.21047

Onoda, K., & Yamaguchi, S. (2013). Small-worldness and modularity of the resting-state functional brain network decrease with aging. *Neuroscience Letters*, *556*, 104–108. https://doi.org/10.1016/j.neulet.2013.10.023

Ouyang, M., Kang, H., Detre, J. A., Roberts, T. P. L., & Huang, H. (2017). Short-range connections in the developmental connectome during typical and atypical brain maturation. *Neuroscience & Biobehavioral Reviews*, *83*, 109–122. https://doi.org/10.1016/j.neubiorev.2017.10.007

Park, H. L., O'Connell, J. E., & Thomson, R. G. (2003). A systematic review of cognitive decline in the general elderly population. *International Journal of Geriatric Psychiatry*, *18*(12), 1121–1134. https://doi.org/10.1002/gps.1023

Righart, R., Schmidt, P., Dahnke, R., Biberacher, V., Beer, A., Buck, D., & Mühlau, M. (2017). Volume versus surface-based cortical thickness measurements: A comparative study with healthy controls and

multiple sclerosis patients. *PLoS One*, *12*(7), e0179590. https://doi.org/10.1371/journal.pone.0179590

Rubinov, M., & Sporns, O. (2010). Complex network measures of brain connectivity: Uses and interpretations. *NeuroImage*, *52*(3), 1059–1069. https://doi.org/10.1016/j.neuroimage.2009.10.003

Seidlitz, J., Váša, F., Shinn, M., Romero-Garcia, R., Whitaker, K. J., Vértes, P. E., Wagstyl, K., Kirkpatrick Reardon, P., Clasen, L., Liu, S., Messinger, A., Leopold, D. A., Fonagy, P., Dolan, R. J., Jones, P. B., Goodyer, I. M., Raznahan, A., & Bullmore, E. T. (2018). Morphometric similarity networks detect microscale cortical organization and predict inter-individual cognitive variation. *Neuron*, *97*(1), 231–247.e7. https://doi.org/10.1016/j.neuron.2017.11.039

Seiger, R., Ganger, S., Kranz, G. S., Hahn, A., & Lanzenberger, R. (2018). Cortical thickness estimations of FreeSurfer and the CAT12 toolbox in patients with Alzheimer's disease and healthy controls. *Journal of Neuroimaging*, *28*(5), 515–523. https://doi.org/10.1111/jon.12521

Shah, C., Liu, J., Lv, P., Sun, H., Xiao, Y., Liu, J., Zhao, Y., Zhang, W., Yao, L., Gong, Q., & Lui, S. (2018). Age related changes in topological properties of brain functional network and structural connectivity. *Frontiers in Neuroscience*, *12*, 318. https://doi.org/10.3389/fnins.2018.00318

Shaw, E. E., Schultz, A. P., Sperling, R. A., & Hedden, T. (2015). Functional connectivity in multiple cortical networks is associated with performance across cognitive domains in older adults. *Brain Connectivity*, *5*(8), 505–516. https://doi.org/10.1089/brain.2014.0327

Shaw, T. G., Mortel, K. F., Meyer, J. S., Rogers, R. L., Hardenberg, J., & Cutaia, M. M. (1984). Cerebral blood flow changes in benign aging and cerebrovascular disease. *Neurology*, *34*(7), 855–862. https://doi.org/10.1212/WNL.34.7.855

Shigemoto, Y., Sato, N., Maikusa, N., Sone, D., Ota, M., Kimura, Y., Chiba, E., Okita, K., Yamao, T., Nakaya, M., Maki, H., Arizono, E., & Matsuda, H. (2023). Age and sex-related effects on single-subject gray matter networks in healthy participants. *Journal of Personalized Medicine*, *13*(3), 419. https://doi.org/10.3390/jpm13030419

Song, J., Birn, R. M., Boly, M., Meier, T. B., Nair, V. A., Meyerand, M. E., & Prabhakaran, V. (2014). Age-related reorganizational changes in modularity and functional connectivity of human brain networks. *Brain Connectivity*, *4*(9), 662–676. https://doi.org/10.1089/brain.2014.0286

Sowell, E. R., Peterson, B. S., Thompson, P. M., Welcome, S. E., Henkenius, A. L., & Toga, A. W. (2003). Mapping cortical change across the human life span. *Nature Neuroscience*, *6*(3), 309–315. https://doi.org/10.1038/nn1008

Sporns, O., & Betzel, R. F. (2016). Modular brain networks. *Annual Review of Psychology*, *67*(1), 613–640. https://doi.org/10.1146/annurev-psych-122414-033634

Taylor, J. R., Williams, N., Cusack, R., Auer, T., Shafto, M. A., Dixon, M., Tyler, L. K., Cam-CAN, & Henson, R. N. (2017). The Cambridge Centre for Ageing and Neuroscience (Cam-CAN) data repository: Structural and functional MRI, MEG, and cognitive data from a cross-sectional adult lifespan sample. *NeuroImage*, *144*, 262–269. https://doi.org/10.1016/j.neuroimage.2015.09.018

Thomas Yeo, B. T., Krienen, F. M., Sepulcre, J., Sabuncu, M. R., Lashkari, D., Hollinshead, M., Roffman, J. L., Smoller, J. W., Zöllei, L., Polimeni, J. R., Fischl, B., Liu, H., & Buckner, R. L. (2011). The organization of the human cerebral cortex estimated by intrinsic functional connectivity. *Journal of Neurophysiology*, *106*(3), 1125–1165. https://doi.org/10.1152/jn.00338.2011

Tijms, B. M., Series, P., Willshaw, D. J., & Lawrie, S. M. (2012). Similarity-based extraction of individual networks from gray matter MRI scans. *Cerebral Cortex*, *22*(7), 1530–1541. https://doi.org/10.1093/cercor/bhr221

Tomasi, D., Wang, G.-J., & Volkow, N. D. (2013). Energetic cost of brain functional connectivity. *Proceedings of the National Academy of Sciences*, *110*(33), 13642–13647. https://doi.org/10.1073/pnas.1303346110

van den Heuvel, M. P., Kahn, R. S., Goñi, J., & Sporns, O. (2012). High-cost, high-capacity backbone for global brain communication. *Proceedings of the National Academy of Sciences*, *109*(28), 11372–11377. https://doi.org/10.1073/pnas.1203593109

van den Heuvel, M. P., & Sporns, O. (2011). Rich-club organization of the human connectome. *The Journal of Neuroscience*, *31*(44), 15775–15786. https://doi.org/10.1523/JNEUROSCI.3539-11.2011

van den Heuvel, M. P., & Sporns, O. (2013). Network hubs in the human brain. *Trends in Cognitive Sciences*, *17*(12), 683–696. https://doi.org/10.1016/j.tics.2013.09.012

Váša, F., Seidlitz, J., Romero-Garcia, R., Whitaker, K. J., Rosenthal, G., Vértes, P. E., Shinn, M., Alexander-Bloch, A., Fonagy, P., Dolan, R. J., Jones, P. B., Goodyer, I. M., the NSPN consortium, Sporns, O., & Bullmore, E. T. (2018). Adolescent tuning of association cortex in human structural brain networks. *Cerebral Cortex*, *28*(1), 281–294. https://doi.org/10.1093/cercor/bhx249

Vértes, P. E., Alexander-Bloch, A. F., Gogtay, N., Giedd, J. N., Rapoport, J. L., & Bullmore, E. T. (2012). Simple models of human brain functional networks. *Proceedings of the National Academy of Sciences*, *109*(15), 5868–5873. https://doi.org/10.1073/pnas.1111738109

Viviani, R. (2013). Emotion regulation, attention to emotion, and the ventral attentional network. *Frontiers in Human Neuroscience*, *7*, 746. https://doi.org/10.3389/fnhum.2013.00746

Wang, H., Jin, X., Zhang, Y., & Wang, J. (2016). Single-subject morphological brain networks: Connectivity mapping, topological characterization and test–retest reliability. *Brain and Behavior*, *6*(4), e00448. https://doi.org/10.1002/brb3.448

Wang, J., Wang, L., Zang, Y., Yang, H., Tang, H., Gong, Q., Chen, Z., Zhu, C., & He, Y. (2009). Parcellation-dependent small-world brain functional networks: A resting-state fMRI study. *Human Brain Mapping*, *30*(5), 1511–1523. https://doi.org/10.1002/hbm.20623

Wang, J., Wang, X., Xia, M., Liao, X., Evans, A., & He, Y. (2015). GRETNA: A graph theoretical network analysis toolbox for imaging connectomics. *Frontiers in Human Neuroscience*, *9*, 386. https://doi.org/10.3389/fnhum.2015.00386

Wang, J.-H., Zuo, X.-N., Gohel, S., Milham, M. P., Biswal, B. B., & He, Y. (2011). Graph theoretical analysis of functional brain networks: Test-retest evaluation on short- and long-term resting-state functional MRI data. *PLoS One*, *6*(7), e21976. https://doi.org/10.1371/journal.pone.0021976

Wang, X., Lin, Q., Xia, M., & He, Y. (2018). Differentially categorized structural brain hubs are involved in different microstructural, functional, and cognitive characteristics and contribute to individual identification. *Human Brain Mapping*, *39*(4), 1647–1663. https://doi.org/10.1002/hbm.23941

Wang, Y., Zhang, Y., Zheng, W., Liu, X., Zhao, Z., Li, S., Chen, N., Yang, L., Fang, L., Yao, Z., & Hu, B. (2022). Age-related differences of cortical topology across the adult lifespan: Evidence from a multisite MRI study with 1427 individuals. *Journal of Magnetic Resonance Imaging*, *57*, 434–443. https://doi.org/10.1002/jmri.28318

Watts, D. J., & Strogatz, S. H. (1998). Collective dynamics of 'small-world' networks. *Nature*, *393*, 440–442. https://doi.org/10.1038/30918

Wu, K., Taki, Y., Sato, K., Kinomura, S., Goto, R., Okada, K., Kawashima, R., He, Y., Evans, A. C., & Fukuda, H. (2012). Age-related changes in topological organization of structural brain networks in healthy individuals. *Human Brain Mapping*, *33*(3), 552–568. https://doi.org/10.1002/hbm.21232

Yin, G., Li, T., Jin, S., Wang, N., Li, J., Wu, C., He, H., & Wang, J. (2023). A comprehensive evaluation of multicentric reliability of single-subject cortical morphological networks on traveling subjects. *Cerebral Cortex*, *bhad178*, 9003–9019. https://doi.org/10.1093/cercor/bhad178

Yotter, R. A., Nenadic, I., Ziegler, G., Thompson, P. M., & Gaser, C. (2011). Local cortical surface complexity maps from spherical harmonic reconstructions. *NeuroImage*, *56*(3), 961–973. https://doi.org/10.1016/j.neuroimage.2011.02.007

Zanto, T. P., & Gazzaley, A. (2013). Fronto-parietal network: Flexible hub of cognitive control. *Trends in Cognitive Sciences*, *17*(12), 602–603. https://doi.org/10.1016/j.tics.2013.10.001

Zhang, T. (2011). Abnormal small-world architecture of top–down control networks in obsessive–compulsive disorder. *Journal of Psychiatry & Neuroscience*, *36*(1), 23–31. https://doi.org/10.1503/jpn.100006

Zhang, Y., Wang, Y., Chen, N., Guo, M., Wang, X., Chen, G., Li, Y., Yang, L., Li, S., Yao, Z., & Hu, B. (2021). Age-associated differences of modules and hubs in brain functional networks. *Frontiers in Aging Neuroscience*, *12*, 607445. https://doi.org/10.3389/fnagi.2020.607445

Zhao, T., Cao, M., Niu, H., Zuo, X.-N., Evans, A., He, Y., Dong, Q., & Shu, N. (2015). Age-related changes in the topological organization of the white matter structural connectome across the human lifespan: Lifespan trajectory of human structural connectome. *Human Brain Mapping*, *36*(10), 3777–3792. https://doi.org/10.1002/hbm.22877

Zhao, T., Mishra, V., Jeon, T., Ouyang, M., Peng, Q., Chalak, L., Wisnowski, J. L., Heyne, R., Rollins, N., Shu, N., & Huang, H. (2019). Structural network maturation of the preterm human brain. *NeuroImage*, *185*, 699–710. https://doi.org/10.1016/j.neuroimage.2018.06.047

Ziegler, G., Dahnke, R., Jäncke, L., Yotter, R. A., May, A., & Gaser, C. (2012). Brain structural trajectories over the adult lifespan. *Human Brain Mapping*, *33*(10), 2377–2389. https://doi.org/10.1002/hbm.21374

Zuo, X.-N., He, Y., Betzel, R. F., Colcombe, S., Sporns, O., & Milham, M. P. (2017). Human connectomics across the life span. *Trends in Cognitive Sciences*, *21*(1), 32–45. https://doi.org/10.1016/j.tics.2016.10.005

Zuo, X.-N., Kelly, C., Di Martino, A., Mennes, M., Margulies, D. S., Bangaru, S., Grzadzinski, R., Evans, A. C., Zang, Y.-F., Castellanos, F. X., & Milham, M. P. (2010). Growing together and growing apart: Regional and sex differences in the lifespan developmental trajectories of functional homotopy. *The Journal of Neuroscience*, *30*(45), 15034–15043. https://doi.org/10.1523/JNEUROSCI.2612-10.2010

SUPPORTING INFORMATION

Additional supporting information can be found online in the Supporting Information section at the end of this article.

How to cite this article: Ruan, J., Wang, N., Li, J., Wang, J., Zou, Q., Lv, Y., Zhang, H., & Wang, J. (2023). Single-subject cortical morphological brain networks across the adult lifespan. *Human Brain Mapping*, *44*(16), 5429–5449. https://doi.org/10.1002/hbm.26450